Project Report On

Synthesis and Characterization of alternative cathode material, $LiMn_2O_4$ for lithium ion batteries by solid state and sol-gel route

Submitted By

Divya Singh (2K13/NST/19)

In partial fulfillment of requirements for the award of the degree in

M.Tech (Nano Science &Technology)

(2013-2015)

Under the Guidance of

Dr. Amrish K. Panwar

Assistant Professor

Department of Applied Physics

Delhi Technological University

Shahbad Daulatpur, Delhi – 110042

DELHI TECHNOLOGICAL UNIVERSITY

CERTIFICATE

This is to certify that **Divya Singh (Roll No. 2K13/NST/19)** has successfully completed Project on "**Synthesis and Characterization of alternative cathode material $LiMn_2O_4$ for Li-ion batteries by solid state and sol-gel route"** in partial fulfillment of the requirements of the M.Tech in Nano Science & Technology of Delhi Technological University under the supervision and guidance of **Dr. Amrish K. Panwar, Assistant Professor**, Department of Applied Physics, DTU.

……..

……

Dr. Amrish K. Panwar
Assistant Professor
Dept. of Applied Physics.
DTU

Prof. S. C. Sharma
HOD
Dept. of Applied Physics
DTU

DECLARATION

I hereby declare that the work presented in this dissertation entitled **"Synthesis and Characterization of alternative cathode material $LiMn_2O_4$ for Li-ion batteries using sol-gel and Solid State Route"**, has been carried out by me under the guidance of **Dr. Amrish K. Panwar, Assistant Professor** and hereby submitted for the partial fulfillment for the award of degree of Master of Technology in Nanoscience and Technology at Applied Physics Department, Delhi Technological University (Formerly Delhi College of Engineering), New Delhi.

I further undertake that information and data enclosed in this dissertation is original and has not been submitted to any University/Institute for the award of any other degree.

…….

Divya Singh
(2K13/NST/19)
M.Tech.(Nanoscience & Technology)
Delhi Technological University
Delhi.

ACKNOWLEDGEMENT

I gratefully acknowledge my indebtedness to my project guide **Dr. Amrish K. Panwar** , my M.Tech coordinator Dr**. Pawan K. Tyagi** , our HOD **Prof. Suresh C. Sharma,** research scholar **Mr. Aditya Jain** and **Mr. Rakesh Saroha** for their cooperation and suggestions during the preparation of this project work. Our teachers have been a great source of inspiration for us who has given the ideas related to our project topic and most of their ideas and suggestions have been incorporated in this report. Some of my classmates proved to be a great source of information in finalizing the project topic from concept to finishing of the project. I express my deep gratitude to the friends and teachers for their co-operation, suggestions and comments.

Divya Singh

(2K13/NST/19)

M.Tech.(Nanoscience & Technology)

Delhi Technological University

TABLE OF CONTENTS

CHAPTER-2-LITRATURE REVIEW

CHAPTER-3-SYNTHESIS AND CHARACTERIZATION OF $LiMn_2O_4$

LIST OF FIGURES

ABSTRACT

The key to success in the development of advanced Lithium ion batteries (LIBs) to meet the emerging EV market demands is the electrode materials, especially the cathode. The cathode costs nearly twice as much as the anode. This could be attributed to the fact that the working voltage, energy density, and rate capability of a LIB are mainly determined by the limited theoretical capacity and thermodynamics of the cathode material in the present LIB technology. $LiMn_2O_4$ spinel is one of the most promising alternative cathode material for LIBs due to its low cost, environmental friendliness, good safety, higher electrochemical potential vs. graphite, and its improved thermal stability. In this work, synthesis of spinal LMO with the help of solid state and sol-gel routes has been carried out. Further the physio-chemical characterizations are performed such as SEM, EDS, XRD, Conductivity measurement, I-V characteristics of LMO, and Activation energy calculation for LMO prepared by both the routes to optimize the properties of $LiMn_2O_4$ in terms of good cyclability, capacity and power density during the electrochemical analysis of batteries.

Chapter1
Introduction

1.1 Elementary battery concepts:

A battery is a device which converts chemical energy into electrical energy by using an electrochemical reduction-oxidation reaction. Mainly, there are two types of batteries: primary and secondary batteries. In primary batteries, the electrode reactions are irreversible & the cells are therefore not rechargeable, which means after one discharge, they are discarded. In secondary batteries, the electrode reactions are reversible & the cells are rechargeable. Any battery comprises three main components that are cathode, electrolyte and anode. Cathode is described as the electrode where a reduction-reaction occurs *(*which means electrons are accepted from an outer circuit), whereas an oxidation-reaction occurs at the anode (which means electrons are donated to an outer circuit). Electrolyte is an electronic insulator, but it is a good ionic conductor. Its main function is providing a transport-medium for ions to move from one electrode to another. It also necessarily prevents short-circuiting by acting as physical barrier between the electrodes, either alone(in the case of a polymer) or in the matrix it impregnates (the separator) if a liquid. Voltage and capacity of a cell are the functions of electrode materials used.

1.2 Need for Li ion batteries (Why Li ion batteries??)

In the 21st century, Environment and energy based issues have become the major areas of concern because these factors are directly related to technological development; that's why the search for alternative sources of energy is still continue. In the present time energy economy, which is based on fossil fuels, is at risk because of the decrement in non-renewable resources & the continuously increasing demand for energy. Also, CO_2 emissions associated with the fossil fuels are one of the main causes for global warming, and this is becoming an important issue in global energy politics. In Accordance to it, investments for exploitation of

renewable energy sources are increasing worldwide, with a particular attention to wind, solar and battery power systems.

The Batteries have a lot of advantages as an alternative source for energy storage mechanism. As it has no moving parts or noise and without any pollution, batteries are able to convert chemical energy directly into electrical energy. They require a little upkeep for large-scale applications. Presently, the conventional battery technologies, for ex. lead-acid and nickel cadmium batteries, are slowly being replaced by lithium-ion batteries, fuel cell technologies and nickel metal hydride batteries. Lithium ion battery technology comes out as a forerunner and market leader as compared to the other energy systems. The main motivation behind using this Lithium ion battery technology is that lithium is the most electropositive and the lightest metallic element, therefore it has a very high energy density. Lithium ion batteries are found to be stable over 500 cycles. They can be fabricated in various sizes and also require little maintenance compared to the other battery technologies. The Researchers continue to work on various aspects of this technology like decreasing the cost, increasing the safety and improving the cycling life. The Li-ion technology is also being used in high end electronics and recently introduced to the power tool markets. Now, it is entering the hybrid electric vehicle market hence making it a serious competition for the power electric cars of the future time. Lithium ion batteries are used in cameras, calculators, cardiac pacemakers and other implantable devices. These batteries are also used in telecommunication equipments, portable radios & TVs, pagers etc. They are used in mobile phones, laptop computers and aerospace applications.

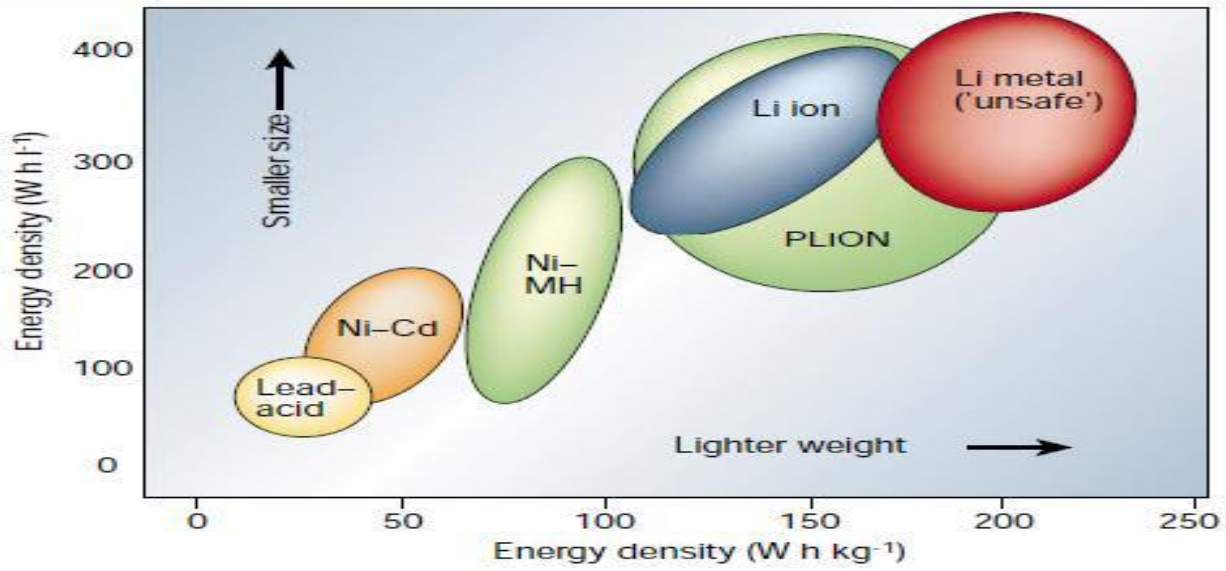

	Lead-Acid	Ni-Cd	Ni-MH	Li-ion
Cell voltage (V)	2	1.2	1.2	3.6
Specific energy (Wh/kg)	1-60	20-55	1-80	3-100
Specific power (W/kg)	< 300	150 – 300	< 200	100 – 1000
Energy density (kWh/m^3)	25-60	25	70-100	80-200
Power density (MW/m^3)	< 0.6	0.125	1.5 – 4	0.4 – 2
Maximum cycles	200-700	500-1000	600-1000	3000
Discharge time range	> 1 min	1 min-8 hr	> 1 min	10 s-1 h
Cost ($/kWh)	125	600	540	600
Cost ($/kW)	200	600	1000	1100
Efficiency (%)	75 - 90	75	81	99

Fig 1.1 Comparison of various battery technologies

The highlighting features of commercial Lithium ion batteries are:

1. High operating potential ; a single cell has an average operating voltage of approx. 3.6 V, which is three times the operating voltage of Ni-Cd and Ni-MH batteries & twice the operating voltage of sealed Pb-acid batteries.
2. These batteries are Compact, lightweight, and high energy density i.e. the energy density is about 1.5 times & specific energy is about twice as compared to the high-capacity Ni-Cd batteries.
3. They have fast charging potential as batteries can be charged upto 80-90% of full capacity in one hour duration.
4. High discharge rate are attainable.

5. A wide range of operating temperature ranging from –20 to $+60^0$C.

6. Excellent cycle life; service life of a battery exceeds 500 cycles.

7. Excellent safety: United States Department of Transportation, Dangerous Materials Division declared Li-ion batteries exempt from dangerous materials regulations.

8. Low self discharge: only 8-12% per month.

9. Long shelf-life: no reconditioning required up to approximately 5 years (Ni-Cd: 3 months; Ni-MH: 1 month).

10. No memory-effect: can be recharged at any time.

11. Non- polluting: does not use toxic heavy metals such as Pb, Cd or Hg.

1.3 Charging and discharging procedure:

An electrical battery is one or more electrochemical cells that convert stored chemical energy into electrical energy. There are two major types of batteries: **primary and secondary**. Primary batteries are those which cannot be recharged because the chemical reaction inside the battery cannot be reversed and once used it must be discarded. Secondary batteries can be recharged and can be reused multiple times. A Li-ion battery usually refers to a secondary battery in which energy is stored chemically through red-ox reactions that employ lithium intercalation between the positive (cathode) and the negative (anode) electrodes i.e. as a battery is charged and discharged the lithium ions move back and forth between the cathode and the anode . Because of this they are also referred as "Rocking-chair" batteries. Basically there are four primary components of a lithium-ion battery: the anode, cathode, separator and electrolyte for which a variety of materials may be used. The cathode acts as a positive electrode which accepts the electrons while reducing and the anode acts as a negative electrode which donates the electrons and oxidizes during the discharge cycles. The electrodes do not touch each other but are electrically connected by the electrolyte while the separator prevents the mixing between them but allows ions to flow.

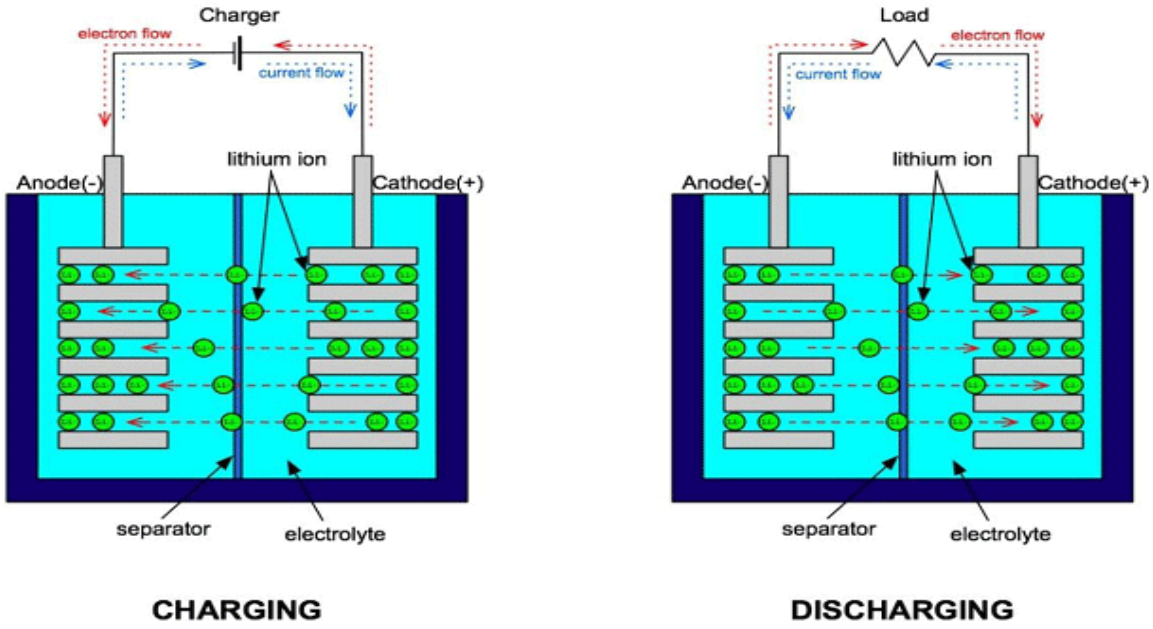

Figure1.2: Electrode and cell reactions in a Lithium Ion battery

To understand this process briefly we can consider the example of a standard LiCOO2 battery in which LiCOO2 acts as a cathode. During charging, lithium ions move from cathode to anode and electrons are removed from cathode by an external field and then transferred to anode. During discharge, anode supplies the ions to electrolyte and electrons to the external circuit where the ions intercalate into cathode and electrons move from the external circuit for charge compensation. This red-ox reaction is shown below.

Positive: $LiMO_2 \underset{\text{discharge}}{\overset{\text{charge}}{\rightleftharpoons}} Li_{1-x}MO_2 + xLi^+ + xe^-$

Negative: $C + xLi^+ + xe^- \underset{\text{discharge}}{\overset{\text{charge}}{\rightleftharpoons}} Li_xC$

Overall: $LiMO_2 + C \underset{\text{discharge}}{\overset{\text{charge}}{\rightleftharpoons}} Li_xC + Li_{1-x}MO_2$

1.4 Limitations and scope:

All technologies have their advantages and disadvantages. Lithium ion technology is no different. Like the use of any technology, there are some disadvantages that need to be balanced against the benefits. The Li-ion battery disadvantages include:

Protection required: Lithium ion cells and batteries are not as robust as some other rechargeable technologies. They require protection from being over charged and discharged too far. In addition to this, they need to have the current maintained within safe limits. Accordingly one lithium ion battery disadvantage is that they require protection circuitry incorporated to ensure they are kept within their safe operating limits. Fortunately, with modern integrated circuit technology, this can be relatively easily incorporated into the battery, or within the equipment if the battery is not interchangeable.

Ageing : One of the major lithium ion battery disadvantages for consumer electronics is that lithium ion batteries suffer from ageing. Not only is this time or calendar dependent but also dependent upon the number of charge discharge cycles that the battery has undergone. When a typical consumer lithium cobalt oxide, LCO battery or cell needs to be stored it should be partially charged - around 40% to 50% and kept in a cool storage area. Storage under these conditions will help increase the life.

Transportation : Another disadvantage of lithium ion batteries is that there can be certain restrictions placed on their transportation, especially by air. Although the batteries that could be taken in aircraft carry-on luggage are unlikely to be affected, care should be taken not to carry any more lithium ion batteries than are needed. Any battery carried separately must be protected against short circuits by protective covers etc.

Cost: A major lithium ion battery disadvantage is their cost. Typically they are around 40% more costly to manufacturer than nickel cadmium cells. This is a major factor when considering their use in mass produced consumer items where any additional costs are a major issue.

Immature Technology : Lithium ion battery technology is a developing area. This can be a disadvantage in terms of the fact that the technology does not remain constant. However as new lithium ion technologies are being developed all the time, it can be an advantage as better solutions are coming available.

1.5 Different Cathode Materials:

Although the efficiency of energy conversion for LIBs depends on a variety of factors, their overall performance strongly relys on the structure and property of the materials used. The key to success in the development of advanced LIBs to meet the emerging EV market demands is the electrode materials, especially the cathode. The cathode costs nearly twice as much as the anode. This could be attributed to the fact that the working voltage, energy density, and rate capability of a LIB are mainly determined by the limited theoretical capacity and thermodynamics of the cathode material in the present LIB technology. As discussed in more details below, therefore, it is critical to develop promising cathode materials for the current LIB technology.

(1)In the past two decades, the layered oxide $LiCOO_2$ cathode has been widely used in portable electronics. The high cost, toxicity, chemical instability in the deep charged state, safety concern, and limited capacity(only 135 Ah/ kg) associated with $LiCOO_2$, however, have prevented its large-scale applications in transportation and stationary storage. LiCOO2 is not as stable as other potential electrode materials and can undergo performance degradation or failure when overcharged. Stoichiometric $LiCOO_2$ can be difficult to obtain, so heat treatment to control the surface phase content is needed to improve performance during cycling.

$LiNiO_2$ is lower in cost and has a higher energy density (15% higher by volume, 20% higher by weight), but is less stable and less ordered, as compared to $LiCOO_2$. The lower degree of ordering results in nickel ions occupying sites in the lithium plane, which impedes lithiation / delithiation and also creates challenges in obtaining the appropriate composition.

Having a similar capacity of 140 Ah/kg as that of $LiCOO_2$, but a relatively high working voltage of 4.7V (4.1 V for $LiCOO_2$), $LiMn_{1.5}Ni_{0.5}O_4$ is becoming an attractive candidate for high-energy applications. Furthermore, the cycle life and rate capability of doped $LiMn_{1.5}Ni_{0.5}O_4$ (spinel structure) could be enhanced significantly by cationic substitutions (Co, Cr, Fe, Ga, or Zn) and surface modification($AlPO_4$, ZnO,Al_2O_3 andBi_2O_3).

(2) Lithium-excess layered oxides, $Li[Li, Mn, Ni, Co]O_2$, such as $(Li_2MnO_3)_x(LiMO_2$ (M=Ni, Co, Mn))$_{1-x}$, offer a 4.0 V working voltage with much higher capacity values of 250 Ah/kg than those of $LiCOO_2$ and $LiMn_{1.5}Ni_{0.5}O_2$. However, there is often a huge irreversible capacity loss associated with the oxygen and lithium loss from the host structure of the

lithium-excess layered oxides (Li [Li, Mn, Ni, CO] O_2) at the end of the first charging process. The high surface area associated with the nanostructured lithium-excess layered oxides (Li [Li, Mn, Ni, CO] O_2) could have a high surface reactivity to induce side reactions between the electrodes and the electrolyte . This could lead to destabilization of the active materials and an increase in impending passivation. Therefore, the electrolyte safety, together with the relatively high cost of the electrode materials, is the major concern for lithium-excess layered oxides to be used as the cathode in LIBs.

(3) Another promising cathode material is $LiMn_2O_4$ that forms a spinel structure (Fd3m), in which manganese occupies the octahedral sites and lithium predominantly occupies the tetrahedral sites. $LiMn_2O_4$, is lower cost and safer than $LiCOO_2$, but has a lower capacity. One of the challenges in the use of $LiMn_2O_4$ as a cathode material is that phase changes can occur during cycling. Other transition metals, including iron and cobalt, have been added to $LiMn_2O_4$. The capacity increases with increasing manganese content and a 3:1 Mn:Ni ratio (i.e. $Mn_{1.5}Ni_{0.5}O_4$) is the most commonly used composition .The manganese and nickel cations can order on the octahedral sublattice, but a disordered spinel structure has been shown to have a higher capacity. Partial substitution of cobalt for nickel (i.e. $Li[Mn_{1.42}Ni_{0.42}Co_{0.16}]O_4$) has been used to reduce the formation of $Li_xNi_{1-x}O$, which can degrade cell performance during cycling .The addition of nickel to the surface of $LiMn_2O_4$ through coatings, rather than as a bulk dopant, can also be effective in improving capacity retention during cycling.

(4) Another promising class of cathode material are phosphates ($LiMPO_4$) with the olivine structure (Pnma), in which phosphorous occupies tetrahedral sites, the transition metal (M) occupies octahedral sites and lithium forms one-dimensional chains along the [0 1 0] direction. The phosphate most commonly used for the cathode is $LiFePO_4$. $LiFePO_4$ been recently developed for commercial applications because of its low cost, low toxicity, high safety and excellent cycling performance. Mixtures of phosphates, including $LiMnPO_4$ or $LiCOPO_4$with $LiFePO_4$, have been used for cathode materials. In such mixtures, the operating voltage increases with increasing manganese content, while capacity increases with increasing iron content.

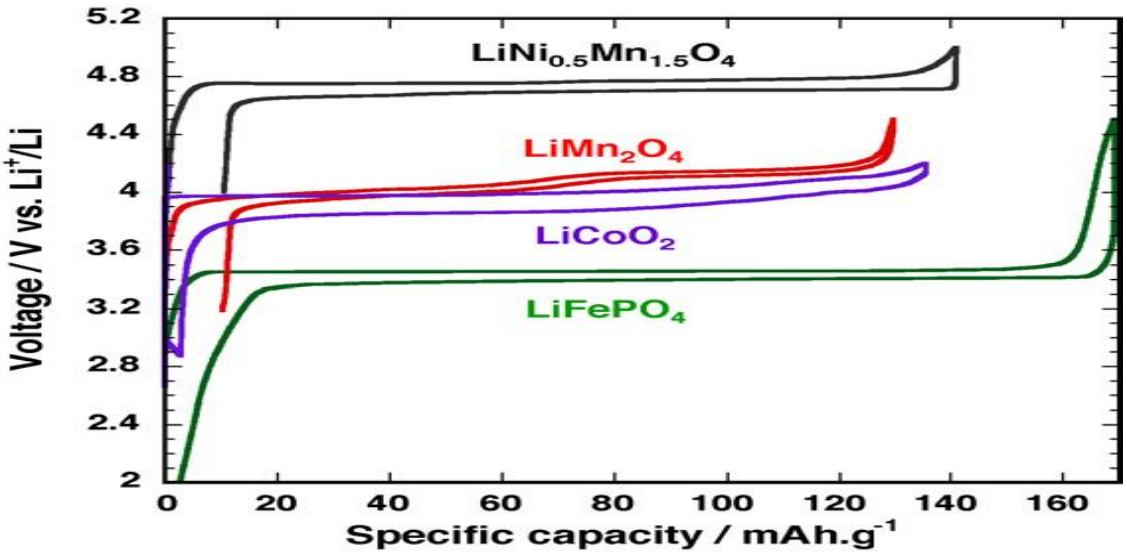

Fig 1.3: Performance comparison of various cathode materials

(5) Compared with the cathode materials described above, Li–O_2, Li–S/C, and Li_2S–Si can offer a much higher energy density, which is a distinguished advantage that could make them the most promising cathode material. For the Li–O_2 battery, however, the reversibility and compatibility are still big problems, as well as the catalysts for the O_2 cathode. For the Li–S/C and Li_2S–Si battery systems, the cycling life and polarization of the nanostructured sulphur also need to be further improved.

1.6 $\underline{LiMn_2O_4}$:

$LiMn_2O_4$ spinel as one of the most promising cathode materials attracts extensive attention, due to its low cost, environmental friendliness, good safety, higher electrochemical potential vs. graphite, and its improved thermal stability . $LiMn_2O_4$ with different morphologies, including nanowires, nanospheres, nanotubes, nanorods, nanoparticles, nanochains, double-shelled hollow microspheres and hollow nanofibers, and composites with graphene or carbon nanotubes have been prepared by spray pyrolysis, template-based reaction, a modified resorcinol–formaldehyde route, hydrothermal, solvothermal, sol–gel, electrospinning, ball-milling and molten salt methods, and have been systematically investigated for their applications in Li-ion batteries.

1.6.1 Structure & Properties:

Fig.2 shows the schematic diagram of lattice atom group of $LiMn_2O_4$. The structure of $LiMn_2O_4$ belongs to the face centre cubic lattice and each lattice is made up of 2 lithium atoms, 4 manganese atoms and 8 oxygen atoms . In contrast to the layered oxides ($LiCOO_2$ or $LixMyCOyO_2$, M = Ni, Mg, Ti) presently used in commercial Li-ion cells $LiMn_2O_4$ adopts a (3D) structure that can simply be described as a cubic close packing (ccp) of oxygen atoms with Mn occupying half of the octahedral and Li an eighth of the tetrahedral sites referring to the 16d and 8a sites ($[Li]_{tet}$ $[Mn_2]_{Oct}$ O_4), respectively. However, this structure is complicated by possible cations mixing between two types of sites. It is well documented that, within the spinel family, the degree of cations mixing and extent of cationic or anionic non stoichiometry affecting the spinel magnetic or optical properties is strongly dependent on the thermal story of the sample. Thus, it was important to first determine whether or not the Li intercalation / deintercalation process within $LiMn_2O_4$ was sensitive to the sample history (precursors, heat--treatments) and subsequent cation mixing as the early electrochemical data suggested. In the $LiMn_2O_4$ spinel structure (space-group: Fd3m), a ccp array of oxygen ions occupy the 32e position, Mn ions are located in the 16d site and Li in the 8a site. The Mn ions have an octahedral coordination to the oxygens, and the MnO_6 octahedral share edges in a three dimensional host for the Li guest ions. The 8a tetrahedral site is situated furthest away from the 16d site of all the interstitial tetrahedral (8a, 8b and 48f) and octahedra (16c). Each of the 8a-tetrahedron faces is shared with an adjacent, vacant 16c site. This combination of structural features in the stoichiometric spinel compound constitutes a very stable structure.

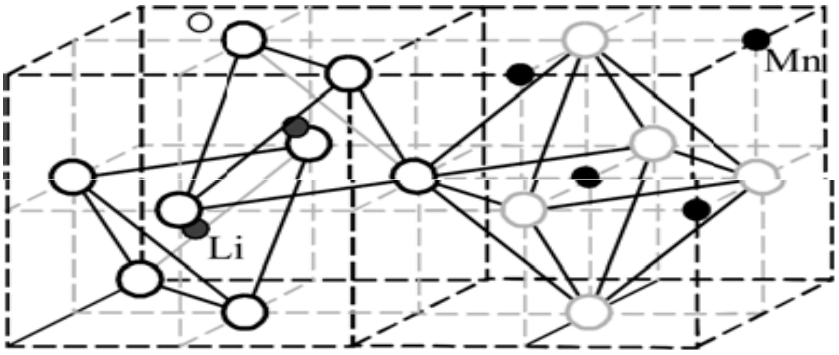

Fig.1.4 Schematic diagram of lattice atom group

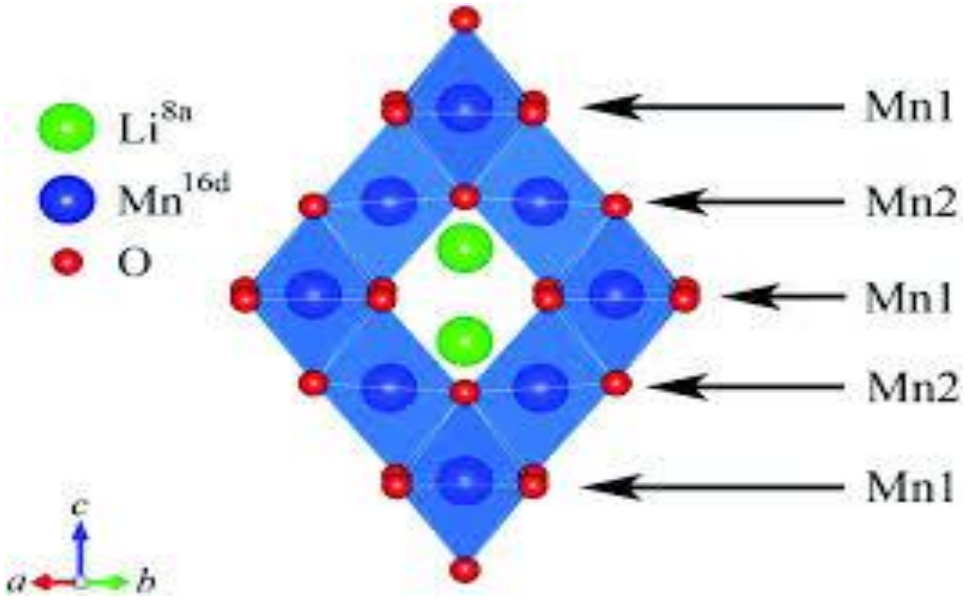

Fig1.5 The spinel structure showing *the MnO6* octrahedra and the Li 8a tetrahedral positions

1.6.2 As a cathode material:

$LiMn_2O_4$ is ideal as a high-capacity Li-ion battery cathode material by virtue of its low toxicity low cost and the high natural abundance of Mn. Unlike V_2O_5 and LiV_3O_8, lithium can be extracted from $LiMn_2O_4$ in the form it is made qualifying $LiMn_2O_4$ as a positive electrode material for Li-ion batteries. $LiMn_2O_4$ is a leading positive electrode material alternative to $LiCOO_2$ due to its lower cost, slightly higher electrochemical potential and its improved thermal stability. High power applications such as electric vehicles require that Li-ion batteries have a high specific power and energy. One route to increase specific power is to significantly increase the interfacial area between electrochemically active material and electrolyte, thereby increasing the charge and discharge rates. This opportunity has led many groups to develop nano-structured and/ or nanosized $LiMn_2O_4$ particles with promising results.

$LiMn_2O_4$ was first synthesized is 1958 by heating a mixture of lithium carbonate and manganese oxide at 850^0C in air. The theoretical specific capacity of $LiMn_2O_4$ is 148 mAh/g and the practical specific capacity approaches to 120 mAh/g. For some applications, however, a capacity of about 120 mAh/ g is acceptable, provided the value remains stable under extended charge-discharge cycling. During de-intercalation, lithium ions leave the

spinel $LiMn_2O_4$ structure and this leads to the formation of Mn_2O_4 in which the spinel structure is retained. It is supposed that lithium ions can be intercalated fully from the host structure and that the structure does not deteriorate as in case of $LiNiO_2$ and $LiCOO_2$ when lithium ions are extracted. These merits make $LiMn_2O_4$ an ideal material, in principle, for use in large scale batteries for powering electric vehicles (EV) or hybrid electric vehicles (HEV), but the energy density of LIBs is still too low to support their practical application. Fabrication of high energy density LIBs requires a cathode material with high specific capacity and high density.

1.6.3 Limitations & Scope:

One big disadvantage of $LiMn_2O_4$ cathodes is the well-known dissolution of Mn, which has been known to be caused by the disproportionation of Mn^{3+} generating soluble Mn^{2+}. The surface orientations of $LiMn_2O_4$ supporting Li diffusion are especially vulnerable to the dissolution of Mn3, making both high-rate capability and a long lifetime very difficult to achieve simultaneously. This issue could be addressed by developing a truncated octahedral structure. It enables excellent rate performance and cycle life simultaneously by truncating a small portion of surfaces along the (1 1 0) orientations to support Li diffusion while leaving most remaining surfaces aligned along the (1 1 1) orientations with minimal dissolution of Mn^{3+}. The truncated octahedral structure exhibits superior performance in both rate capability and cycle life than the control structures with smaller dimensions.

High power applications such as electric vehicles require that Li-ion batteries have a specific power and energy. One route to increase specific power is to significantly increase the interfacial area between electrochemically active material and electrolyte thereby increasing the charge and discharge rates. This opportunity has led many groups to develop nanostructured and nanosized $LiMn_2O_4$ particles with promising results. $LiMn_2O_4$ with different morphologies, including nanowires, nanospheres, nanotubes nanorods, nanoparticles, nanochains, double-shelled hollow microspheres are prepared.

In $LiMn_2O_4$ nanosized systems, synthetic procedures are generally complex, cost affected and difficult to scale up. A number of soft chemistry techniques such as sol-gel, solution phase, combustion, and templating methods have been explored to prepare $LiMn_2O_4$. Moreover, electrochemical performance of the electrode materials are closely associated with the preparation methods. $LiMn_2O_4$ prepared by the traditional solid state reaction method exhibits good performance but it requires prolonged high temperature

(calcinations) of 800ºC, which causes coarsening of the powders. Thus, a simple and convenient route to synthesize $LiMn_2O_4$ nanostructures without loss of electrochemical properties is highly desired. A tartaric acid method was developed to synthesize nano $LiMn_2O_4$ powder directly from lithium acetate and manganese acetate. Without using other chemicals (such as glycol, ammonium hydroxide, ammonium chloride or polyhydric alcohol) and additional processing steps, this synthesis method was considered to be inexpensive and simple.

1.7 Synthesis Methods:

A number of soft chemistry techniques such as sol-gel, solution phase, combustion, and templating methods have been explored to prepare $LiMn_2O_4$. Moreover, electrochemical performances of the electrode materials are closely associated with the preparation methods. Here, we synthesized $LiMn_2O_4$ from two different routes, i.e., solid state reaction method and sol-gel method. A brief introduction of these methods is given in this section.

1.7.1 Solid state method:

The solid state reaction route is the most widely used method for the preparation of solids from a mixture of solid starting materials. Solids do not react together at room temperature over normal time scales and it is necessary to heat them to much higher temperatures in order for the reaction to occur at an appreciable rate. Products from solid state reactions are always thermodynamically stable compounds. The factors on which the feasibility and rate of a solid state reaction depend, include, reaction conditions, structural properties of the reactants, surface area of the solids, their reactivity and the thermodynamic free energy change associated with the reaction. Solid state reactions are usually slow (from 8 hours to several days) due to large amount of structural reorganization bonds break and ions migrate through a solid. The reaction occurs much more quickly with increasing temperature.

Solid state reaction will not occur until the temperature reaches at least 2/3 of the melting point of reactants. Some problems may also occur during this process such as evaporation of a reactant due to high temperature and reaction of a reagent with the container. Some other disadvantages associated with this method include long duration, poor chemical homogeneity, large grain size, use of high temperatures, lack of control of products formed. Some advantages are also there such as, starting material readily available, compounds can be prepared in large amounts and easy to carry out the synthesis procedure.

1.7.2 Sol-gel method:

Sol-gel methods are promising candidates to prepare cathode materials owing to their evident advantages over traditional methods. The prepared products provide better electrochemical performance including reversible capacity, cycling behaviour and rate capability in comparison with those from traditional solid-state reactions. The main reasons are due to the following several factors such as homogeneous mixing at the atomic or molecular level, lower synthesis temperature, shorter heating time, better crystallinity, uniform particle distribution and smaller particle size at the nanometer level. As a result, the structural stability of the cathode materials and lithium intercalation and deintercalation behaviour are much improved. With further development and application of sol-gel methods, better and new cathode materials will become available and the advance of lithium ion batteries will greatly promoted Current research on cathode materials for lithium ion batteries is very active and many preparation methods have been widely explored, such as incorporation of heteroatoms, composite technology , soft chemistry routes including ion exchange, hydrothermal and oxidation–reduction reactions , some non classical methods such as mechano-chemical methods, template methods, pulsed laser deposition, plasma-enhanced chemical vapour deposition, radiofrequency magnetron sputtering and sol-gel methods. Among them, sol-gel methods are promising since they have many advantages over conventional solid-state reactions such as homogeneous mixing at the atomic or molecular level, good stoichiometric control, low synthesis temperature, short heating time, good crystallinity, uniform particle size and small diameter, even at the nanometer level. The basic processing steps of this method can be summarized as follows:

Precursor – hydrolysis – reactive monomer – condensation – sol gelation –gel-further treatment

Since long range diffusion is not required for these sol-gel methods, unlike the solid state reaction method, a single spinel phase of $LiMn_2O_4$ can be obtained at a low temperature such as 250–300^{0}C .sol-gel methods are important to improve the electrochemical properties of cathode materials for lithium ion batteries. With spinel-type lithium manganese oxides, the degree of disordering of the cation distribution in the crystal lattice is greatly circumvented due to good mixing hence the Jahn–Teller effect is alleviated. In addition, the stability of the spinel structure is increased and dissolution of Mn^{2+} is decreased owing to effective doping

and coating. Consequently, the cycling behaviour is greatly improved. After coating, the rate capability is also improved. With the development of sol-gel methods in combination with other technologies, new and better cathode materials with unique properties may become available, Moreover, one main advantage of the sol-gel methods is the possibility to prepare nano-materials, which become more and more important in science and technology. In the near future, a lot of nano cathode materials will be prepared, and microbatteries will come into use for application in microelectronic devices such as microsatellites, providing promising applications for cathode materials prepared by sol-gel methods.

Chapter-2

Literature Review

2.1 Structural Analysis:

Most of the commercial Li-ion batteries use layered Li (Ni, Co, Mn) O_2 and spinel type $LiMn_2O_4$ (working at 4V) as cathode & graphite as anode material. $LiMn_2O_4$ was extensively investigated by many groups as a 4 V cathode material [1,2,3]. Among most of the cathode materials, spinel materials have a structural advantage. These materials have a general formula AB_2O_4 & here the oxygen atoms occupy 32e site (Fd3m space group) and form a FCC close packing. 'A' cations occupy tetrahedral 8a site, while the B cations are located in the octahedral 16d sites. The unoccupied octahedral 16c site with the 8a tetrahedral site forms a 3-dimensional pathway for lithium diffusion in these materials.

This type of easy lithium diffusion is hindered in case of inverse spinels due to the displacement of half of the Li-ions on the 8a site by the metal ions from the 16d site [1]. The reaction at 4 V is highly reversible; however, the reaction at 3 V leads to Jahn-Teller distortion, which causes irreversible structural damage. Hence, in most cases, deep discharge is avoided in order to ensure better reversibility [1]. To prevent Jahn–Teller distortion, $LiMn_2O_4$ are only used below 4V vs. Li/Li^+ with a limited practical capacity of around 140mAh/g (the theoretical capacity of $LiMn_2O_4$ is 148mAh/g. Furthermore, the material exhibits a very good cycling stability at RT but shows very severe capacity fading at elevated temperatures [1,4] which is mainly associated with Mn^{2+} dissolution from the structure as a result of the disproportionation reaction. The above mentioned drawbacks can be overcome to a certain extent by doping $LiMn_2O_4$ with metal ions, especially of 3d transition metals and in most cases, the doping results in a higher operating voltage [5-13]. The addition of iron results in an additional discharge plateau at high voltages, while cobalt improves the capacity retention during cycling by stabilizing the spinel crystal structure. However, the most common addition to $LiMn_2O_4$ is nickel [15], which decreases the lattice parameter and the electrical conductivity of $LiMn_2O_4$ [16]. The capacity increases with increasing manganese content and a 3:1 Mn:Ni ratio (i.e. $Mn_{1.5}Ni_{0.5}O_4$) is the most commonly used composition

[17,18]. The manganese and nickel cations can order on the octahedral sublattice, but a disordered spinel structure has been shown to have a higher capacity [19].

The addition of nickel to the surface of $LiMn_2O_4$ through coatings, rather than as a bulk dopant can also be effective in improving capacity retention during cycling [20–22]. $LiMn_2O_4$ is usually obtained by calcination of mixtures of oxides, carbonates, or hydroxides at high temperatures (700–800^{0}C) for 24–48 hr in air [23,24]. The stoichiometric $LiMn_2O_4$ obtained by calcination reveals regular structure in Fd3m space group with the lattice constant (a) of 0.82495(2) nm [25]. It was reported in a previous work that the Li–Mn spinel sample obtained by an alternative sol-gel method and further calcined at 800^{0}C in air showed the lattice constant equal 0.82517(7) nm [26]. It is thought that the higher value of the lattice constant is related to more homogenous and stoichiometric spinel. The stoichiometric $LiMn_2O_4$ shows a reversible phase transition from cubic to orthorhombic structure around room temperature (290^0 K). This transformation is affected by Jahn–Teller distortion of high spin Mn^{3+} ions [27,28] with accompanying columnar charge ordering in the manganese sublattice, so called electronic crystallization [29]. Such behaviour is responsible for the decrease of the cell capacity upon cycling [30, 31]. It is possible to suppress the phase transition by partial substitution of Mn^{3+} by 3d metal ions (Cr, Ni, Co, Fe, Cu) [32–36] or Al^{3+} [37]. In addition, the insertion of lithium excess in octahedral 16d (in place of Mn3C) sites in spinel structure stabilizes that structure [38, 39]. Each of the possibilities mentioned above changes the Mn^{3+}/Mn^{4+} ratio due to the substitution of Mn^{3+} and/or charge compensation. This is the reason for disappearance of the phase transition, as it appears only if the Mn^{3+}/Mn^{4+} ratio is within 1–1.18 [37]. Substitution of 3d metal ions into manganese sublattice changes the character of discharge curves [36, 40].

In recent work Paolone et al. [41] reported a thermal decomposition of spinel samples during collection of Raman spectra due to laser heating. The authors used very strong radiation (500 KW/cm^2) at 632.8 nm, which is near resonance band. They suggested that the correct Raman spectrum of $LiMn_2O_4$ should consist of a broad peak at 580 cmK^{-1} with two poorly defined features between 300 and 400 cmK^{-1}. However, at 625 cmK^{-1} Ammundsen et al. [42] have found narrow band that was ascribed to totally symmetric vibration. The same was reported by Julian et al. [43]

2.2 Electrochemical Performance:

Spinel $LiMn_2O_4$ has become the most attractive cathode material for transportation and large-scale batteries due to its low cost, environmental friendliness, good structural stability, and much improved safety. As discussed previously, $LiMn_2O_4$ adopts the spinel structure with space group Fd3m in which the Li and Mn occupy the 8a tetrahedral and16d octahedral sites of the cubic close-packed oxygen ions, respectively. The edge-shared octahedral Mn_2O_4 host structure is highly stable and possesses a series of intersecting tunnels formed by the face-sharing of tetrahedral lithium (8a) sites and empty octahedral (16c) sites. Such tunnels allow the three-dimensional diffusion of lithium. The lithium intercalation / deintercalation into / from the 8a tetrahedral sites occurs at about 4V with the maintaining of the initial cubic spinel symmetry. Surplus lithium can be intercalated into the spinel $LiMn_2O_4$ to reach a maximum composition of $Li_2Mn_2O_4$, which occurs at about 3V against the lithium anode with a phase transformation from cubic to tetragonal phase. The cubic to tetragonal phase transition, often referred to as Jahn–Teller distortion, is accompanied by a 6.5% increase in the unit cell volume, which damages the structural integrity of the electrode during charge/discharge cycling and results in rapid capacity fading [44]. To prevent Jahn–Teller distortion, $LiMn_2O_4$ are only used below 4V vs. Li/Li^+ with a limited practical capacity of around 140 mAh/g (the theoretical capacity of $LiMn_2O_4$ is 148 mAh/g while the theoretical capacity of $Li_2Mn_2O_4$ is 296mAh/g). However, $LiMn_2O_4$ tends to exhibit capacity fading even in the 4V region, especially at elevated temperatures. Several detrimental effects, including Jahn–Teller distortion at the surface of the particles under conditions of non equilibrium cycling [45], dissolution of Mn into the electrolyte [46], formation of two cubic phases in the 4Vregion [47], loss of crystallinity [48], and development of micro-strain [49] during cycling, could be the source of the capacity fading Several strategies have been developed to overcome the detrimental effects, such as cationic substitutions that results in $LiM_yMn_{2-y}O_4$ (M¼Li,Cr,Co,Ni,andCu) and the surface modification. However, these strategies usually cause decrease in capacity. On the other hand, the reduction of particle size is a promising strategy since it can alleviate these detrimental effects (except for the case of dissolution of Mn) and also improve the electrochemical performance of $LiMn_2O_4$.

The power density of lithium-ion batteries is limited by the low rate capability of the electrode materials. In particular, the slow lithium ion and and electron diffusion in the cathode materials lead to insufficient lithium ion insertion/extraction under

high charge/discharge rates [50]. Two methods are generally employed to increase the rate capability of the cathode materials. One method is to reduce the crystallite size and particle size of the cathode materials from micrometer to nanometer so that the electron and lithium ion diffusion paths can be shortened [51]. Another method is to add conductive additives to the cathode materials to improve their electrical conductivity [52].

Yunjian Liu, Xinhai Li studied about the Electrochemical performance and capacity fading reason of $LiMn_2O_4$ cathode Li-ion batteries stored at room temperature. They observed discharge capacities of $LiMn_2O_4$/graphite before and after storage are 106.8 and 102.8mAhg−1, respectively. The ratio of capacity recovery after storage is 96.3%. That is to say that 3.7% capacity of battery is lost during the storage with half charged at room temperature for 28 days without cycling. It is well known that the capacity fading during storage is commonly linked to the Mn dissolution also shows that the cyclic performances of $LiMn_2O_4$ battery were improved with the cycle proceeding. This can be concluded that the amount of Li^+ inserting the $Li_xMn_2O_4$ is low because of the decreased discharge capacity, which results in higher value of Mn in the $Li_xMn_2O_4$ and diminishing the Li^+ concentration in the vicinity of the material surface. So the Jahn-Teller distortion is restrained and results in better cyclic performance. The surface of $LiMn_2O_4$ is eroded badly by electrolyte during storage. The SEM images also indicate that the $LiMn_2O_4$ electrode reacts with electrolyte and results in Mn dissolution during the storage. The intensity of all peaks in the XRD patterns of the $LiMn_2O_4$ electrode were depressed after storage The dissolution of Mn is generally attributed to the existence of HF, which is easily formed in the case of using $LiPF_6$ as the electrolyte salt. The correlation of HF formation and Mn dissolution was experimentally reported [53]. $LiPF_6$ itself contains a small amount of HF during the manufacturing process, and the salt can easily react with water to form HF. Thus HF unavoidably exists with very low concentration in the electrolyte, as shown in Li's paper [54]. The combination of HF–H_2O in the presence of air is known to react on the $LiMn_2O_4$ in an aqueous medium, according to the following equation [55]:

$$2LiMn_2O_4 + 4H^+ \rightarrow 3\alpha\text{–}MnO_2(s) + Mn^{2+}(l) + 2Li^+(l) + 2H_2O \qquad (1)$$

MnO_2 is vice production of the Mn dissolution according the Equation (1). The solid state MnO_2 should be deposited on the surface of $LiMn_2O_4$ electrode, and separates the $LiMn_2O_4$

electrode from the electrolyte. So it will be good to the electrochemical performance. The Mn^{2+} is reduced and deposited on the anode surface, according to the following equation:

$$Mn^{2+} + 2e^- \rightarrow Mn \quad \text{..... (2)}$$

The resistance and polarization of $LiMn_2O_4$/electrolyte are increased because of the covered MnO_2. Mn dissolution and the increase of Li-ion migration resistance for $LiMn_2O_4$/electrolyte surface are mainly responsible for capacity loss. The deposited MnO_2 film increases the Li-ion migration resistance of $LiMn_2O_4$/electrolyte after storage, but it also separates the $LiMn_2O_4$ from electrolyte, which improves the cyclic performance.

2.2.1 Synthesis Methods:

2.2.1.1 Co-precipitation method:

The researches show that the properties for lithium-ion battery cathode materials are affected by materials selection, chemical proportion and controllable conditions during the experimental course [56,57]. Using co-precipitation method, the advantages of synthesizing spinel $LiMn_2O_4$ are the evenly compositions of precipitation within atom size order, overcoming the disadvantages of long-cycle and high-energy exhausting with solid-phase method, and lowering synthesis cost. Moreover, the product has well-scattered particle, regular appearance, and developed crystal phase [58]. Ming Shu Zhao∗, Xiao Ping Song studied about this and performed an experiment. They observed that there are two endothermic peaks and two exothermic peaks existed during the decomposition process of lithium manganese oxide precursor at dynamic air atmosphere under four different heating rates of 8, 10, 15 and 20Kmin−1. Using DTA and XRD measurements, decomposition process of lithium manganese oxide precursor could be divided into three stages of dehydration, decomposition and synthesis. The apparent active energies of four peaks are calculated. The average values are 69.831, 165.093, 326.128, 645.983 kJ mol−1, respectively. On the basis of DTA experiments and kinetics calculations, lithium manganese oxide was prepared using '**carbonate co-precipitation method'** and sintering method, and the result is a pure phase, well-distributed particle and has regular appearance with spinel structure.

2.2.1.2 Sol-gel method:

Ting-Feng Yia et al. prepared a series of $LiMn_2O_4$ spinel by adipic acid-assisted' **sol–gel'** method at different temperatures and The structure and physicochemical properties were investigated The spinel phase $LiMn_2O_4$ calcined at 800 ◦C has higher crystallinity, better ordering of local structure, and lower lattice strain. The crystallites size increase with increasing in sintering temperature, and $LiMn_2O_4$ spinel powder with various particle sizes can be obtained by controlling the sintering temperature. Mn oxidation state in $LiMn_2O_4$ spinel decrease with increasing synthesized temperature. The average chemical valence of Mn element of the samples calcinated 800 ◦C is most close to 3.5, which has the least lattice defect. The capacity retention sintered at 350, 700 and 800^0C over the first 50 cycles is 93.6%, 86.1% and 85.2%, respectively, but the discharge capacity is 82.2, 104.8 and 110.8mAhg−1, respectively. $LiMn_2O_4$ spinel powders calcined at higher temperatures have high discharge capacity and capacity loss, and sintered at lower temperatures has low discharge capacity and high capacity retention. Among them, $LiMn_2O_4$ powder formed about 800^oC presents the best electrochemical activity.

H. Liu,Y. P. Wu, E. Rahm, R. Holze, H. Q. Wu suggested that thin film $LiMn_2O_4$ electrodes can be prepared by a solgel method using spin coating and annealing processes with anhydrous manganese acetylacetonate and lithium acetylacetonate as precursors. Electrochemical properties of the film electrode depend on the drying temperature, even when subjected to the same annealing conditions. The discharge capacity of the annealed film increases with the drying temperature. However, the rate of capacity fading during cycling also increases with the drying temperature [60]. The electrochemical performance of the prepared $LiMn_2O_4$ is much improved in comparison with that from the solid-state reaction [61, 62]. For example, the reversible capacity is up to 135 mAh/g (91% of theoretical capacity) and the capacity fading is very slow. With lithium metal as a reference electrode, after 168 cycles the capacity fades only 9.5%. The enhancement in capacity in comparison with solid-state reactions can partly be ascribed to the smaller particles from sol-gel methods , since the diffusion path for lithium ions is shorter and the change in the volume to surface area of individual particles during charge–discharge cycling is smaller . The highly crystalline phase is the main cause $LiMn_2O_4$ can also be prepared directly from heating a gelatinous $LiMn_2O_4$ powder obtained by drying a sol from lithium acetate dihydrate, manganese acetate tetrahydrate and tartaric acid at 50^0C . Amorphous and crystalline spinel materials can be obtained. It is found that the chemical diffusivity of lithium ions in the

amorphous powder electrode specimen is nearly constant at about 10)8 cm^2/s, irrespective of the lithium content in the 0.45–0.7 range at room temperature, and 10 times higher than that in the crystalline material. The improvement in electrochemical performance by sol-gel methods can be mainly ascribed to the marked decrease in disordering of Li^+ and $Mn3^+$ due to the low HTT and short heat-treatment time, short diffusion path from a small particle size, and the high-purity spinel phase of $LiMn_2O_4$. In addition, sols can be used to prepare thin-film electrodes by spin coating and dip coating, which cannot be easily achieved by solid-state reactions.

2.2.1.3 <u>Solid state route</u>:

Xianyan Zhou et al. prepared Spinel $LiMn_2O_4$ cathode material by‘ **solid-state combustion synthesis**’ based on a two-stage calcination progress which used lithium carbonate and manganese carbonate as raw materials and citric acid as a fuel. The structure and physicochemical properties of the obtained $LiMn_2O_4$ powders were investigated. Here the temperature of the second stage plays a key role in the structure and physicochemical properties of the obtained $LiMn_2O_4$ products. During the successful synthesis progress of $LiMn_2O_4$, the weight loss occurs in three temperature regions. When further calcinations temperature was performed lower than 700 ^oC, the diffraction peaks of all the combustion products are identified as a single phase of cubic spinel structure with the space group Fd3m. Compared with other conditions, the as-prepared $LiMn_2O_4$ powders which experienced the second-stage, and calcined at 700^oC is the most uniform, and the charge transfer resistance (Rct) is the lowest, accompanying the best electrochemical activity and highest discharge capacity. Its initial discharge specific capacity is 119.1 mAh/g and the discharge capacity retention remains 87.2% after 50 cycles. A comparison of solid-state combustion reaction sample B_{700} and the solid-state reaction sample C700 at the same calcination temperature and time displays better electrochemical performance. Meanwhile, a comparison of sample B700 and the traditional solid-state reaction of Fu et al. [59] reported in their paper shows Spinel $LiMn_2O_4$ powders can be obtained by the solid state combustion method in a short time. Therefore, this method is time and energy saving, and is promising for commercial application.

Cancan Peng et al. prepared $LiMn_2O_4$ via solid-state combustion synthesis using oxalic acid as a fuel. Oxalic acid was used as an assistant fuel to synthesize spinel type $LiMn_2O_4$ by a

simple and efficient solid-state combustion synthesis at 500 °C for 1 h. The influence of the amount of fuel on the physicochemical properties of the products is discussed in detail. XRD patterns reveal that the main phase of the material is spinel $LiMn_2O_4$. SEM images indicate that the as-synthesized LiMn2O4 without oxalic acid consists of agglomerated clusters; however, the products obtained upon the addition of oxalic acid are uniformly distributed spherical-like particles with a clear surface boundary and a slightly reduced particle size. Electrochemical results show that the $LiMn_2O_4$ electrode containing 5 wt% oxalic acid exhibits the highest initial discharge capacity of 108.5 mAh/g. Both the CV and EIS tests also indicate that the specimen containing 5 wt% oxalic acid possesses superior electrochemical reversibility and optimal electrochemical activity.

2.3 Doping/Coating/Surface modification:

The development of improved cathode materials is a challenge for meeting current and future energy storage requirements. Several transition metal based cathode materials can provide high voltages and good capacities. Full utilization of these materials for numerous recharging cycles and at high discharge currents continues to be a challenge. Specifically, stabilizing the desired crystal structure, especially during delithiation, and preventing reaction with the electrolyte are important for long operational life, while improved transport to and in the electrode are important for achieving high discharge current. Progress has been made by engineering the electrode composition, microstructure and morphology.

The performance of cathode materials can be improved by doping, but the interpretation of doping effects can be complicated by the interrelations between doping and microstructure and morphology, since the microstructure formed can be affected by the dopant additions. Chromium forms compounds with the spinel structure and has been added to $LiMn_2O_4$. Chromium reduces the ordering of lithium ions in $LiMn_2O_4$, which stabilizes the single phase spinel structure [56], and has been shown to increase the capacity retention during cycling for spinel electrode materials, including $LiMn_2O_4$. Stability of $LiMn_2O_4$ over a temperature range of battery operation can be obtained by doping with even 10 mol% of chromium. Electrical conductivity values for the various compositions are found to be of the order of ~10-5 S/cm. The discharge capacity becomes ~80 mAh/g for the dopant concentration of x= 0.5.

The beneficial effect of zinc is usually when added in a coating of ZnO where it reduces reaction between the electrode and electrolyte Titanium is also added as a dopant but titanium is beneficial when co-doped with cobalt. Titanium is also added as a TiO_2 coating to reduce electrode dissolution in the electrolyte but degradation of the TiO_2 can lead to degradation in cell performance. Zirconium has similar effects on cathode performance as titanium. Aluminium is a very commonly used dopant in cathode materials. In some cases small amounts of aluminium doping improve the capacity of electrode materials but in most cases the capacity is decreased such as in $LiMn_2O_4$. Aluminum can also be added as an alumina coating and has been shown to improve the capacity and performance at high discharge currents. Magnesium doping has been reported to improve oxide electrodes by modifying the microstructure, or reducing charge transfer resistance , but more often has little, or even a detrimental effect on electrode performance. Fluorine doping has been shown to improve the capacity of spinel cathodes by increasing the lattice parameter and decreasing the average manganese valence. Silver lower in cost than gold and has been shown to improve the performance of $LiCoO_2$, $LiMn_2O_4$ cathodes. The beneficial effect of silver is generally attributed to increased conductivity, but increases in lattice parameter have also been reported in some materials.

Changyin Wang successfully prepared Co and Li doubly doped spinel $LiMn_2O_4$. Compared with undoped spinel, the Co and Li doubly doped spinel exhibits superior capacity retention. The capacity retention of graphite/doped spinel was more than 86% after 1000 cycles at room temperature, and maintained 85% after 100 cycles at 55◦C. The differential capacity profiles on doped spinel cathode are much more fixed than undoped spinel cathode. Mn dissolution into electrolyte at 55 ◦C was reduced by 41%, the lattice parameter difference *a* was reduced by 82% on doped spinel cathode after cycling. We conclude that the greatly enhanced cycling performance is attributed to slow down of manganese dissolution in spinel cathode and stabilize the spinel structure during cycling.

2.4 Progress on spinel cathodes:

The spinel $LiMn_2O_4$ can deliver a high energy density comparable to $LiCOO_2$ thanks to its high voltage and high specific capacity which is only 10% less than that of $LiCOO_2$. It also possesses the essential advantages of lower toxicity and much lower cost. Hence, it has drawn a lot of attention for its use as a 4 V cathode in Li-ion batteries. $LiMn_2O_4$ with different

morphologies, including nanowires, nanospheres, nanotubes, nanorods, nanoparticles, nanochains, double-shelled hollow microspheres and hollow nanofibers, and composites with graphene or carbon nanotubes have been prepared by spray pyrolysis, template-based reaction, a modified resorcinol–formaldehyde route, hydrothermal, solvothermal, sol–gel, electrospinning, ball-milling and molten salt methods, and have been systematically investigated for their applications in Li-ion batteries. Ultrathin $LiMn_2O_4$ nanowires with a cubic spinel structure were prepared using a simple solvothermal reaction to produce a-MnO_2 nanowires, followed by solid-state lithiation . The as-prepared $LiMn_2O_4$ nanowires with diameters less than 10 nm and lengths of several micrometers exhibited an outstanding rate capability and structural stability. The nanowires delivered a reversible discharge capacity of 125 mAh/g at a current rate of 0.5 C (1 C = 148 mA/g). The discharge capacities remained 102 and 86 mAh/g at much higher rates of 10 C and 20 C, respectively. The $LiMn_2O_4$ nanowires showed almost no capacity fading after 100 cycles at a high current rate of 10 C. Such performances were due to both the favourable morphology and the high crystallinity of the nanowires. One big disadvantage of $LiMn_2O_4$ cathodes is the well-known dissolution of Mn, which has been known to be caused by the disproportionation of Mn^{3+} generating soluble Mn^{2+}. The surface orientations of $LiMn_2O_4$ supporting Li diffusion are especially vulnerable to the dissolution of Mn^{3+}, making both high-rate capability and a long lifetime very difficult to achieve simultaneously. This issue could be addressed by developing a truncated octahedral structure. It enables excellent rate performance and cycle life simultaneously by truncating a small portion of surfaces along the (1 1 0) orientations to support Li diffusion while leaving most remaining surfaces aligned along the (1 1 1) orientations with minimal dissolution of Mn^{3+}. The truncated octahedral structure exhibits superior performance in both rate capability and cycle life than the control structures with smaller dimensions.

Chapter-3

Synthesis and Characterization of $LiMn_2O_4$

This chapter deals with the details of experimental part of the research which includes the materials, synthesis methods adopted and various characterizations to confirm the proper phase formation of $LiMn_2O_4$.

3.1 Experimental work:

3.1.1 Synthesis of LiMn2O4 by solid state method:

The compounds manganese acetate [$Mn(CH_3COO)_2$] (99%) and Lithium Carbonate [Li_2CO_3](99%) of Sigma Aldrich make were used for the synthesis of $LiMn_2O_4$ by solid state method. Stoichiometric amount of these compounds were mixed thoroughly with the help of mortar and pestle. The grinding was carried out for 6 hours using acetone as liquid medium for proper mixing. After grinding, the prepared precursor was calcined at 750^0C for 12 hours in air followed by the slow cooling to the ambient temperature. Finally, the powered form of $LiMn_2O_4$ is observed and collected for further characterization.

3.1.2 Synthesis of LiMn2O4 by sol-gel method:

Manganese acetate [$Mn(CH_3COO)_2$] (99%), lithium hydroxide [LiOH] (99%) and citric acid [$C_6H_8O_7$] (95%) of Sigma Aldrich make were used for the synthesis of $LiMn_2O_4$ by sol-gel route of synthesis. Stoichiometric amount of lithium hydroxide and manganese acetate compounds were used. The cationic ratio of Li:Mn=1:2 were separately dissolved in the de-ionized water and then mixed well with an aqueous solution of citric acid used as chelating agent. Ammonium hydroxide was slowly added to this solution with a constant stirring to control pH between 4 and 6. The resultant solution was heated at about 70-80^0C while being stirred with a magnetic stirrer until a thick gel precursor is obtained. Further, this thick gel is dried in oven at 120^0C for 5 hours to remove moisture and hence obtained the dry mass. Finally, the powder obtained is first decomposed at 600^0C for 3 hours & then calcined at 900^0C for 12 hours to obtain fine black powder of $LiMn_2O_4$. Now, the further characterization is done.

3.1.3 Pellet formation:

The calcined powder of $LiMn_2O_4$ obtained from both the synthesis methods were mixed with PVA binder. Mixing of poly vinyl alcohol powder in 20 ml of distilled water and then stirring of 2 hours is done to get a thick sticky liquid of binder. Few drops (3-4 drops) of this solution are then added to the $LiMn_2O_4$ powder and again grinding is done for some time. This mixture is now pressed into pellets using a hydraulic press applying pressure about 75 KPa. The pellets were then heated at 120^0C for 2 hours. These pellets were then coated with silver paste to form electrodes to measure the conductivity and again heated at 150^0C for 2 hours to remove the moisture.

3.2 Characterization of synthesized $LiMn_2O_4$:

3.2.1 XRD (X-Ray Diffraction) characterization:

The diffraction of X-rays by matter results from the combination of two different phenomena: (a) scattering by each individual atom, and (b) interference between the waves scattered by these atoms. This interference occurs because the waves scattered by the individual atoms are coherent with the incident wave, and therefore between themselves as shown in Fig 3.3.

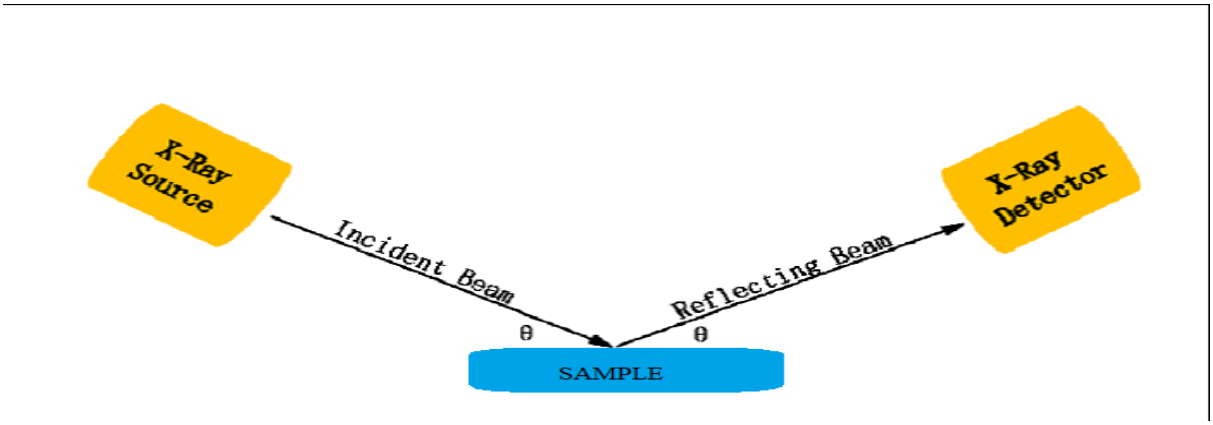

Fig.3.3 Diagram of incident angle and reflecting angle with respect to the normal of the diffracting for X-Ray Diffraction

In 1912, W. L. Bragg recognized a predictable relationship among several factors:

1.The distance between similar atomic planes in a mineral (the inter atomic spacing) which we call the d-spacing and measure in angstrom (Å) .

2. The angle of diffraction i.e. theta angle, measured in degree. Depending on the setting of the combination of θ-2θ, diffractometer measures an angle twice that of the θ angle.

3. The wavelength of the incident X-radiation of Cu-Kα of 1.54 angstrom (Å).

These factors are combined in Bragg's Law:

$$n\lambda = 2d \sin \theta \quad \text{.....(3.1)}$$

where n is an integer, λ is the wavelength of X-rays, d is the lattice inter atomic spacing and θ is the diffraction angle. The XRD was used in this study to identify the crystal structure of the samples prepared by both solid state and sol-gel routes. The powders collected from both the synthesis methods were exposed to X-ray radiation of Cu- Kα of wavelength 1.54 Å. The samples were scanned for a wide range of diffraction angle i.e. from 15^0 to 70^0 at the scan rate of 2 degree/min in a Bruker make D-8 powder diffractometer to get the information about phase formation of $LiMn_2O_4$. The image of the diffractometer used is shown in figure 3.4.

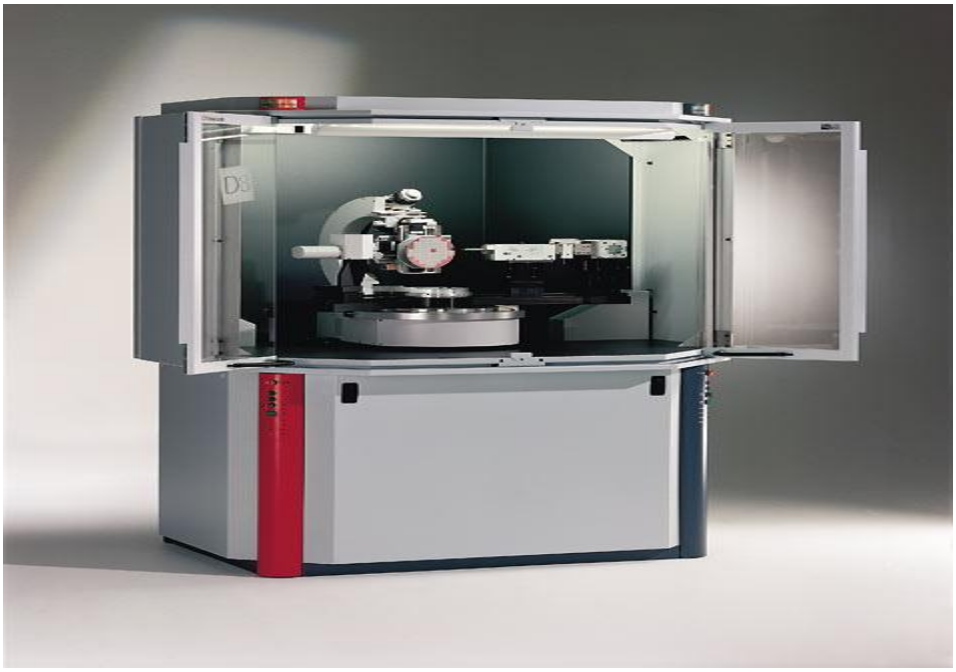

Fig 3.4 Set up used for diffraction pattern

3.2.2 SEM (Scanning electron microscope) observation:

A focused beam of high-energy electrons to generate a variety of signals at the surface of solid specimens is used in the scanning electron microscope (SEM). The signals deriving from electron-sample interactions reveal information about external morphology (texture), chemical composition and crystalline structure and orientation of materials making up the sample. The particle size of the sample is calculated using SEM image. To observe SEM image of synthesized $LiMn_2O_4$ Hitachi make model SN 3700 " scanning image microscope" of maximum resolution 100 nm is used and the micrograph made of secondary emission electrons at different magnifications has been captured at accelerating voltage of 15 KV. The gold coated sample of $LiMn_2O_4$ is mounted and exposed to high energy beam of thermally generated electrons. The intensity of secondary electrons is integrated to observe the shape, size and distribution of existing grain/particle in $LiMn_2O_4$.

3.2.3 EDS (Energy dispersive spectroscopy):

It is also known as energy dispersive X-ray analysis (EDXA) or energy dispersive X-ray microanalysis. This characterization method is mainly used for the elemental analysis of the sample. It works on the fundamental principle that all elements in the periodic table have different atomic structure, and thus they have different set of peaks in x-ray spectrum. Thus with the help of EDS we can identify the elements in any sample. The main disadvantage of EDS is that it does not show any significant peaks for the elements having molecular weight less than 11, i.e. ($Z<11$). For Hydrogen and Helium there are no characteristic x-ray present, and in case of Lithium the emitted x-ray have very low energy such that it can't be detected by the EDS.

Acc.Voltage of 15.0 kV and take Off Angle equal to 74.8 deg is used in this characterization technique.

3.2.4 Conductivity Measurement:

An LCR meter is used for conductivity and dielectric measurements. An LCR meter is a piece of electronic test equipment used to measure the inductance (L), capacitance (C), resistance (R), impedance (Z) of a component. In the simpler versions of this instrument the true values of these quantities are not measured; rather the impedance is measured internally and converted for display to the corresponding capacitance or inductance value. Readings will be reasonably accurate if the capacitor or inductor device under test does not have a

significant resistive component of impedance. More advanced designs measure true inductance or capacitance, and also the equivalent series resistance of capacitors and the Q factor of inductive components. Usually the device under test (DUT) is subjected to an AC voltage source. The meter measures the voltage across and the current through the DUT. From the ratio of these the meter can determine the magnitude of the impedance. The phase angle between the voltage and current is also measured in more advanced instruments; in combination with the impedance, the equivalent capacitance or inductance, and resistance, of the DUT can be calculated and displayed. The meter must assume either a parallel or a series model for these two elements. The most useful assumption, and the one usually adopted, is that LR measurements have the elements in series (as would be encountered in an inductor coil) and that CR measurements have the elements in parallel (as would be encountered in measuring a capacitor with a leaky dielectric). Inductance, capacitance, resistance, and dissipation factor can also be measured by various bridge circuits. They involve adjusting variable calibrated elements until the signal at a detector becomes null, rather than measuring impedance and phase angle.

Bench top LCR meters typically have selectable test frequencies of more than 100 KHz. They often include possibilities to superimpose a biasing DC voltage or current on the AC measuring signal. Lower end meters offer the possibility to externally supply these DC voltages or currents while higher end devices can supply Dc voltage or current internally. In addition bench top meters allow the usage of special fixtures to measure SMD components, air-core coils or transformers.

Aligent make 4284A LCR meter is used to measure resistance and impedance of the samples at room temperature in the frequency range of 20Hz to 1MHz and then corresponding conductivity is estimated using the formula;

$$\mathbf{R = \rho*(L/A)}$$

Where, R = Resistance.

ρ = Resistivity.

σ = Conductivity.

L = Length of the sample, here it would be the thickness of the pellet.

A = Cross sectional area of the sample, here it would be electrode area of the pellet.

3.2.5 I-V Characteristics of the samples:

To measure the I-V characteristics of the prepared sample same pallets were used, in this measurement with the help of electrometer a DC voltage is applied across the pallet, and this voltage is set to change after a short interval of time with the help of DC meter with a step size of .5 volt. As the voltage is keeps on changing the value of the DC current is noted down with the help of DC meter. Modern electrometer is a highly sensitive electronic voltmeter whose input impedance is so high that the current flowing into it can be considered, for most practical purposes, to be zero. The actual value of input resistance for modern electronic electrometers is around $10^{14}\Omega$, compared to around $10^{10}\Omega$ for nano-voltmeters. The measurement of resistance with variation of temperature has been performed with help of Electrometer model 6517.

3.2.6 Activation Energy:

Activation energy is the minimum energy required for a chemical reaction to occur, It can be understood as the potential barrier, which must be reached for a reaction to proceed at a reasonable rate. Arrhenius equation gives the quantitative relation between the rate of reaction and activation energy.

Arrhenius equation is given as;

$\mathbf{k = Ae^{-Ea/RT}}$ **;** where**,** A = Frequency factor, R = Universal gas constant, T = Temperature on Kelvin, k = Reaction rate coefficient, $E_{a.}$ = Activation energy.

Even if we don't know the value of A, we can calculate the value of $E_{a.}$ by calculating the change in reaction rate coefficient with temperature.

The readings were noted down with the 6517 A Electrometer / High Resistance Meter. Now with the help of these readings graph is been drawn with the help of Origin software. The temperature is varied from 30℃ to 200℃.

Chapter-4

Results and Discussion

4.1 XRD Results:

X-ray powder diffraction (XRD) patterns of the powder formed by solid state and sol-gel methods are carried out and shown in figure 4.1. XRD pattern shows that proper phase of $LiMn_2O_4$ is formed from both the routes except the small impurity peak in the sample prepared by solid state route. Both the XRD patterns shows that the Bragg's peaks of $LiMn_2O_4$ are indexed to a cubic system with space group Fd3m in which lithium ions are located in the tetrahedral (8a) sites and Mn ions are located in the 16d sites.

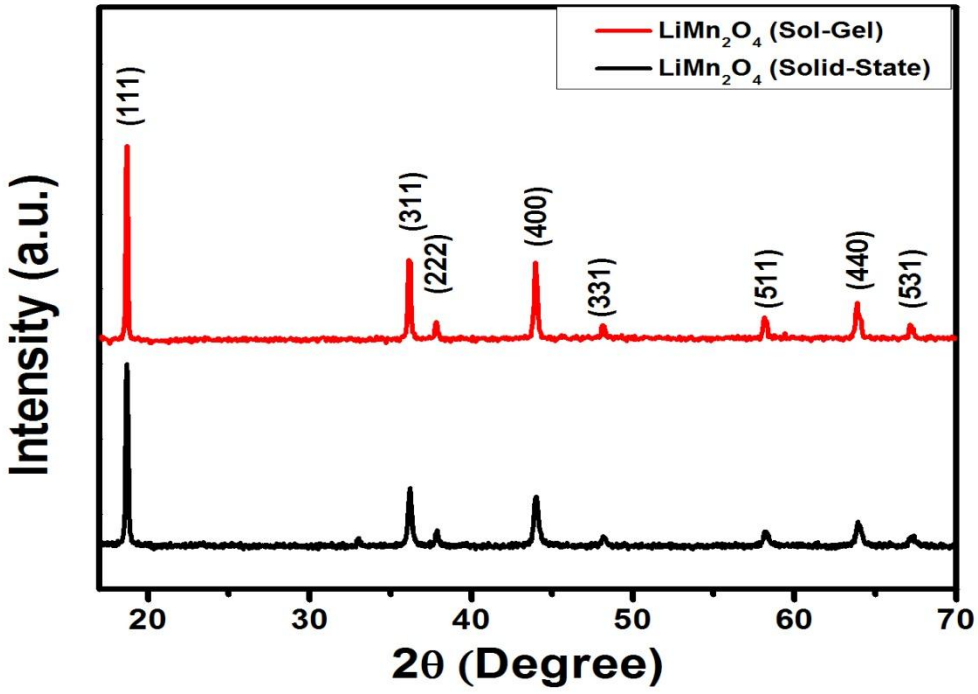

Fig 4.1 XRD pattern for LMO sample prepared by solid state route calcined at 750^{0}C for 12 hours and sample prepared by sol-gel route followed by three stage thermal treatment for 5 hours at 120^{0}C, for 3 hours at 600^{0}C and for 12 hours at 900^{0}C

4.2 SEM images of samples prepared by solid state and sol-gel routes:

The surface morphology, particle distribution and particle size are the important parameter to influence the electrochemical performance. SEM micrographs of $LiMn_2O_4$ sample synthesized by sol-gel and solid state route are shown in figure 4.2 (a), (b), (c) and figure 4.3 (a), (b), (c) at different magnifications. It is observed that $LiMn_2O_4$ prepared by solid state route of synthesis shows regularly distributed particles with non uniform shape of mixed particles in cubic and spherical shapes. The size of particles lies in the range of 200 to 400 nm as can be seen in the figure given below.

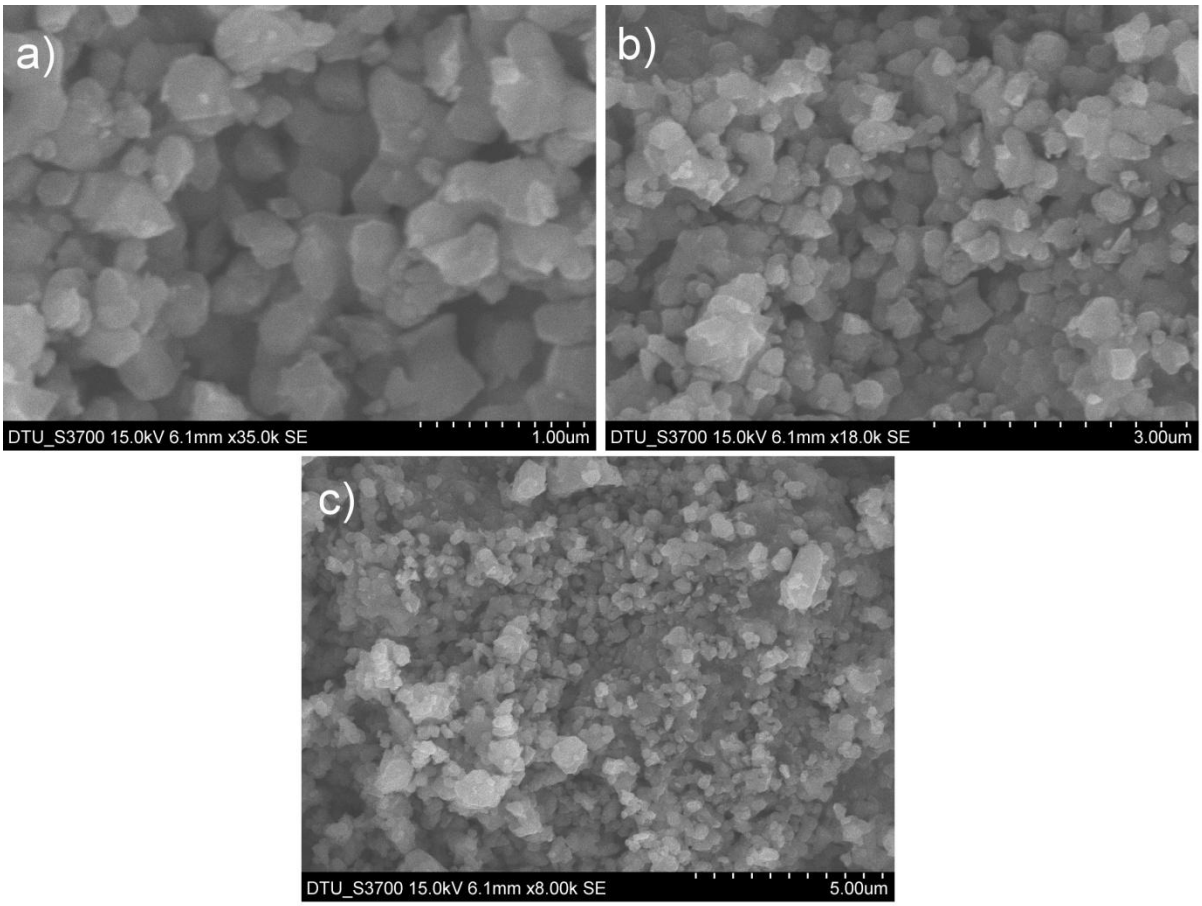

Fig 4.2 SEM images obtained for sample prepared by solid state method calcined at 750^0C for 12 hours at different magnifications (a) at 1 µm (b) at 3 µm (c) at 5 µm

$LiMn_2O_4$ sample prepared by solgel route of synthesis also indicate more regularly distributed particles with uniform cubic shape. The particle of slightly bigger size were formed having their size in the range of 300-500 nm as shown in figure 4.3 (a), (b), (c). Hence SEM results show that sample prepared by solid state route have smaller particle size as compared to the sample prepared by sol-gel route of synthesis.

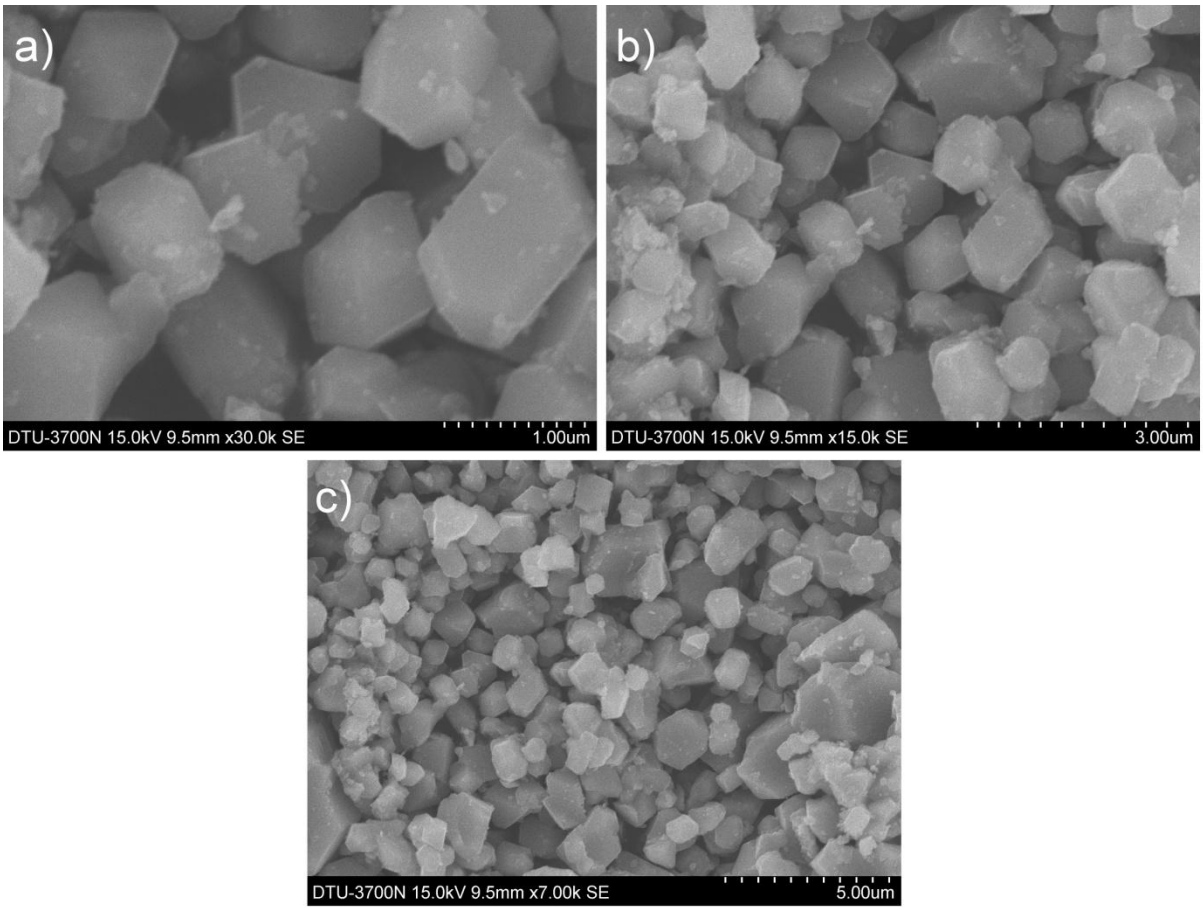

Fig 4.3 SEM images obtained for sample prepared by sol-gel method followed by three stage thermal treatment for 5 hours at 120^0C, for 3 hours at 600^0C and for 12 hours at 900^0C at different magnifications (a) at 1 µm (b) at 3 µm (c) at 5 µm

4.3 EDS Results:

EDS pattern of $LiMn_2O_4$ was observed at accelerating voltage of 15 KV and take off angle 74.8^0. The peaks of Mn and O are clearly visible in the EDS pattern of $LiMn_2O_4$ synthesized by solid state and sol-gel route of synthesis and shown in figure 4.4. The quantitative results obtained from the peaks of pattern is shown in table 4.1. Quantitative results show that Li is absent which is due to lower atomic weight of lithium and it can not be detected by x-ray emission in EDS. Hence weight percent of lithium is added to element Mn to keep the 100 wt% in total. The EDS data also reveals that no impurity peak is observed in $LiMn_2O_4$.

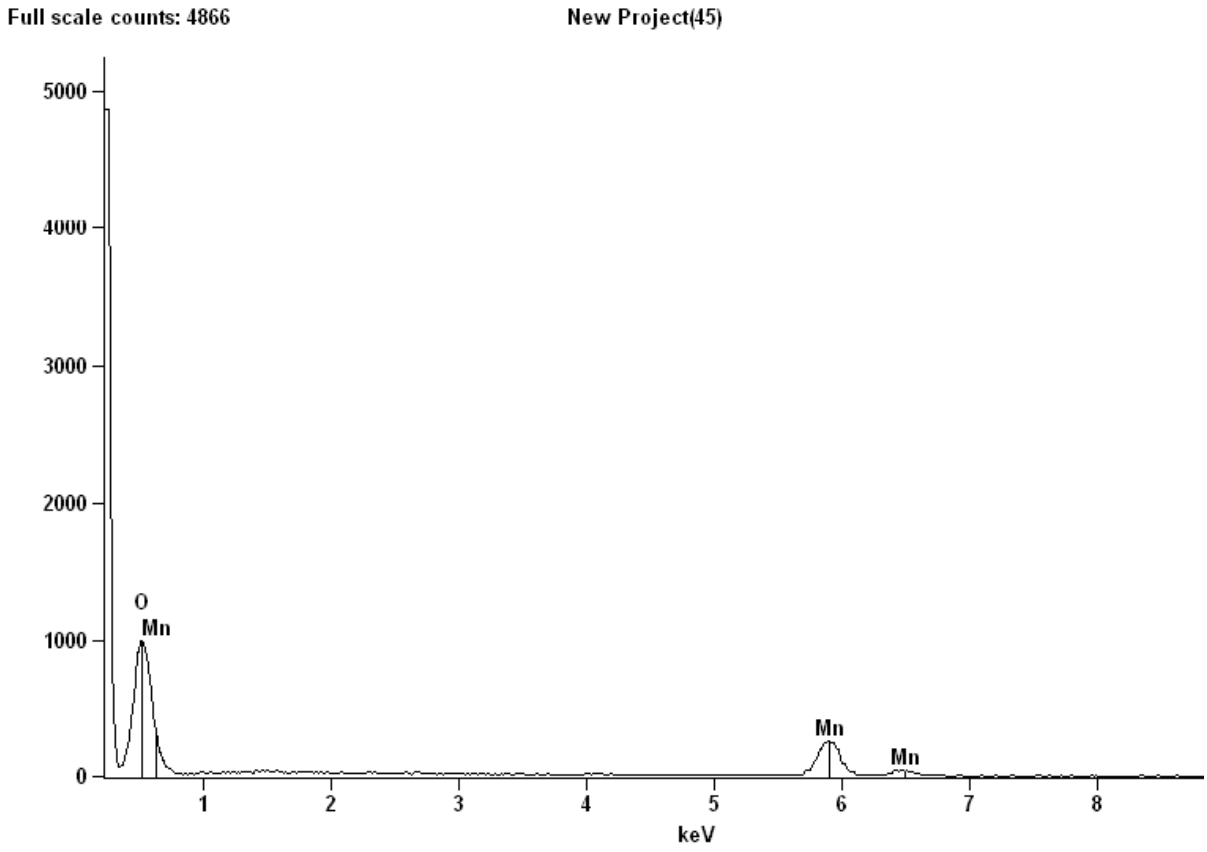

Fig 4.4 EDS pattern of $LiMn_2O_4$

Element Line	Net Counts	Int. Cps/nA	Weight %	Weight % Error	Atom %	Atom % Error	Formula	Standard Name
O K	21501	---	49.76	+/- 0.55	77.28	+/- 0.85	O	
Mn K	5447	---	50.24	+/- 1.41	22.72	+/- 0.64	Mn	
Mn L	4581	---	---	---	---	---		
Total			100.00		100.00			

Table 4.1 Quantitative data of elements in $LiMn_2O_4$ observed by EDS

4.4 I-V characteristics:

I-V characteristics of $LiMn_2O_4$ prepared by both the synthesis methods are shown in figure 4.5 (a) & (b) and measured by electrometer. The DC resistance of $LiMn_2O_4$ samples were calculated using the formula;

DC resistance = slope of the graph = $\Delta V/\Delta I$.

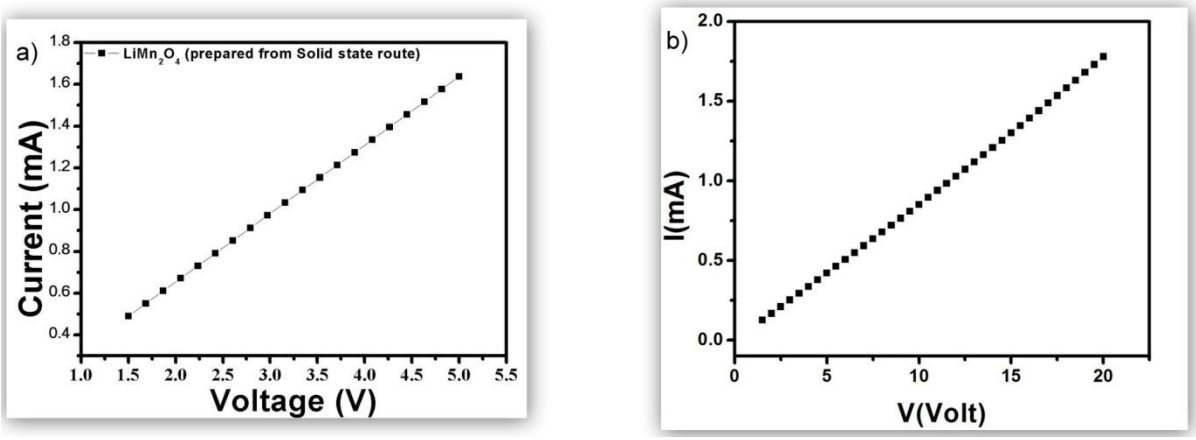

Fig. 4.5 I-V curve of (a) LMO prepared by solid state route calcined at 750^0C (b) LMO prepared by sol-gel route followed by three stage thermal treatment for 5 hours at 120^0C, for 3 hours at 600^0C and for 12 hours at 900^0C

It is observed that DC resistance of $LiMn_2O_4$ prepared by solid state route is calculated as 2.84 KΩ, whereas sample prepared by sol-gel route indicate DC resistance of 11.18 KΩ.

Hence it is clearly visible that $LiMn_2O_4$ sample prepared by solid state route shows less resistance as compared to the sample prepared by sol-gel, and hence better conductivity.

4.5 AC Conductivity measurement:

AC conductivity of both the $LiMn_2O_4$ samples prepared by different synthesis routes has also been measured using the nyquist plot between Z' and Z" and calculated the value of bulk resistance R from semi circle according to the formula;

$$R = \rho*(L/A) \quad \text{.....(4.1)}$$

Nyquist plot for $LiMn_2O_4$ sample prepared by solid state reaction method is shown in figure 4.6 (a). From the plot, it is clear that the value of R is equal to ~ 3 KΩ. On using the dimensions of pellet i.e. thickness 1.33 mm and diameter of pellet equal to 15.28 mm and substituting these values in equation 4.1, the AC conductivity of $LiMn_2O_4$ sample prepared by solid state route is observed as 0.207μS/cm.

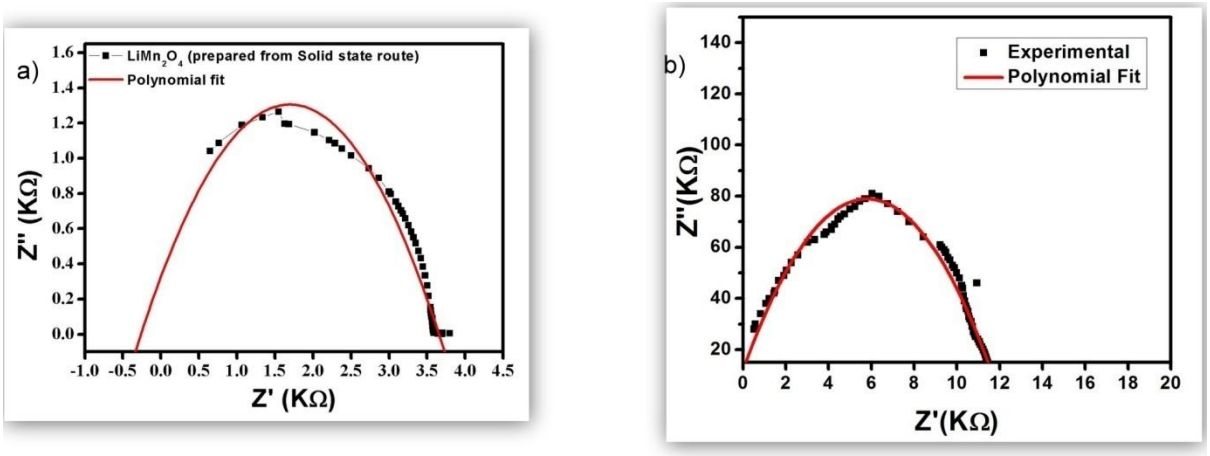

Fig. 4.6 Nyquist plot of (a) LMO prepared by solid state route calcined at 750^0C (b) LMO prepared by sol-gel route followed by three stage thermal treatment for 5 hours at 120^0C, for 3 hours at 600^0C and for 12 hours at 900^0C

Similarly, the AC conductivity of $LiMn_2O_4$ sample prepared by sol-gel route is calculated from the bulk resistance measured from the nyquist plot between Z' and Z" as shown in fig. 4.6 (b) using the dimensions of pellets i.e. thickness 1.49 mm and diameter 10.22 mm. Substituting these values in equation 4.1, the AC conductivity of $LiMn_2O_4$ sample prepared by sol-gel route is observed as 0.151μS/cm. Hence, the AC conductivity of sample prepared by solid state route is more than that of the sample prepared by sol-gel route.

4.6 Activation energy:

Variation of DC conductivity with temperature for $LiMn_2O_4$ samples prepared by solid state and sol-gel route of synthesis are shown in figure 4.7 (a) and (b). Activation energy of both the samples are calculated using the Arhenius equation. It is observed that the sample prepared by solid state route has low activation energy i.e. **441±10 meV** as compared to the activation energy of the sample prepared by the sol-gel route i.e. **491±10 meV** which is a bit higher. Hence it may be concluded that $LiMn_2O_4$ sample prepared by solid state route has more thermal stability.

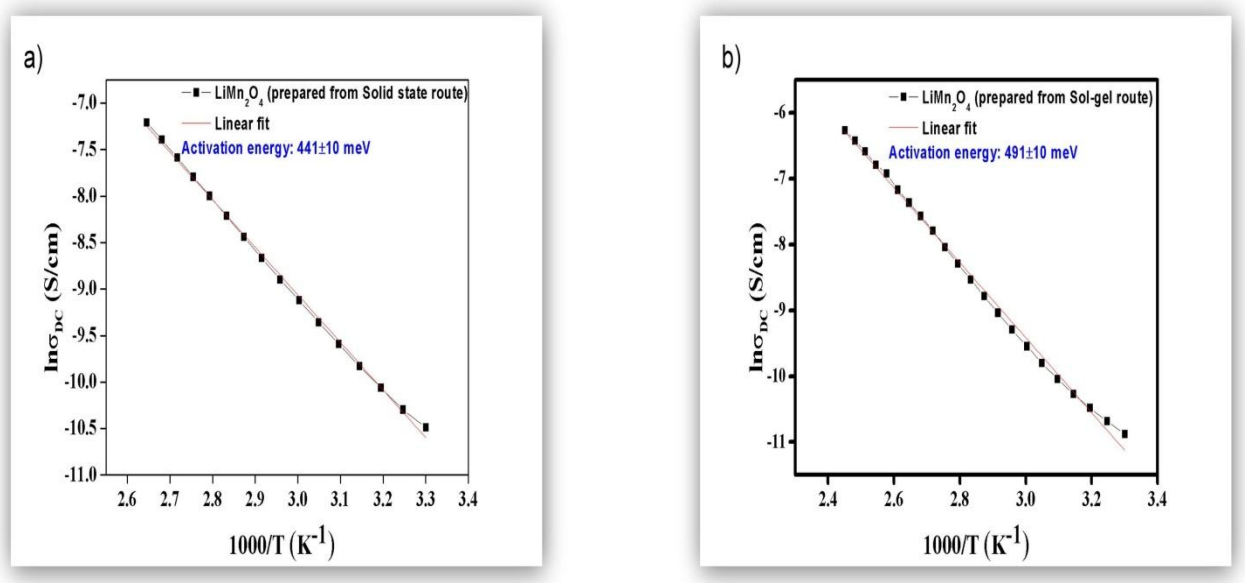

Fig. 4.7 Graph for the Activation Energy calculation for (a) LMO prepared by solid state route calcined at 750^{0}C (b) LMO prepared by sol-gel route followed by three stage thermal treatment for 5 hours at 120^{0}C, for 3 hours at 600^{0}C and for 12 hours at 900^{0}C

Chapter-5
Summary & Conclusion

Synnthesis of proper form of $LiMn_2O_4$ was carried out using two different synthesis methods i.e. solid state reaction method and sol-gel method. XRD characterization indicate the formation of pure phase observed in sol-gel method while there is small secondary peak is observed in solid state reaction route.

SEM results indicate that the regular distributed particles are observed from both the synthesis methods. Solid state route gives the smaller particle size as compared to sol-gel route and the shape of particles are more clear and uniform under sol-gel route.

It is observed that the AC and DC conductivities are improved in $LiMn_2O_4$ sample prepared by solid state route. Similar trend is observed in terms of activation energy as $LiMn_2O_4$ sample prepared by solid state route has lower activation energy as compared to the sample prepared by sol-gel route.

Hence, based on the above characterization, it seems that $LiMn_2O_4$ sample prepared by solid state route may become better alternative cathode material. However, overall Li ion battery performance may be observed by electrochemical analysis which will indicate the better alternative cathode material. The electrochemical analysis of $LiMn_2O_4$ samples is yet to be performed.

ACKNOWLEDGEMENT

.

The work has been supported by Department of Science and Technology (DST), India and Delhi Technological University (DTU), Delhi India.

References

[1]. Thackeray MM. Prog Solid State Chem 1997;25:1.

[2]. Wakihara M, Yamamoto O, editors. Lithium ion batteries: fundamentals and performance. Wiley-VCH; 1998.

[3].Thackeray MM, de Picciotto LA, de Kock A, Johnson PJ, Nicholas VA, Adendorff KT. J Power Sources 987;21:1.

[4]. Gummow RJ, de Kock A, Thackeray MM. Solid State Ionics 1994;69:59.

[5] Amine K, Tukamoto H, Yasuda H, Fujita Y. J Power Sources 1997;68:604.

[6] Kawai H, Nagata M, Tabuchi M, Tukamoto H, West AR. Chem Mater 1998;10: 3266.

[7] Kawai H, Nagata M, Tukamoto H, West AR. J Mater Chem 1998;8:837.

[8] Alcántara R, Jaraba M, Lavela P, Tirado JL. Electrochim Acta 2002;47:1829.

[9] Shigemura H, Sakaebe H, Kageyama H, Kobayashi H, West AR, Kanno R, et al. J Electrochem Soc 2001;148:A730.

[10] Pasero D, De Souza S, Reeves N, West AR. J Mater Chem 2005;15:4435.

[11] Nikolowski K, Bramnik NN, Ehrenberg H. Ionics 2008;14:121.

[12] Jayaprakash N, Kalaiselvi N, Gangulibabu, Bhuvaneswari D. J Solid State Electrochem 2011;15:1243.

[13] Sigala C, Verbaere A, Mansot JL, Guyomard D, Piffard Y, Tournoux M. J Solid State Chem1997;132:372.

[14] T. Ohzuku, S. Takeda, M. Iwanaga, Solid-state redox potentials for Li[Me1/2Mn3/2]O4 (Me: 3d transition metal) having spinel-framework structures: a series of 5 volt materials for advanced lithium-ion batteries, J. Power Sources 81–82 (1999) 90–94.

[15] T.-T. Fang, H.-Y. Chung, Reassessment of the electronic-conduction behaviour above Verwey-like transition of Ni2+- and Al3+-doped LiMn2O4, J. Am. Ceram. Soc. 91 (1) (2008) 342–345.

[16] S. Patoux, L. Daniel, C. Bourbon, H. Lignier, C. Pagano, F. Le Cras, S. Jouanneau, S. Martinet, High voltage spinel oxides for Li-ion batteries: From the material research to the application, J. Power Sources 189 (2009) 344–352.

[17] N.-E. Sung, Y.-K. Sun, S.-K. Kim, M.-S. Jang, In situ XAFS study of the effect of dopants in Li1+xNi(1−3x)/2Mn(3+x)/204 (0≤x≤1/3), a Li-ion battery cathode material, J. Electrochem. Soc. 155

[18] K.M. Shaju, P.G. Bruce, Nano-LiNi0.5Mn1.5O4 spinel: a high power electrode for Li-ion batteries, Dalton Trans. 40 (2008) 5471–5475.

[19] J. Liu, A. Manthiram, Understanding the improvement in the electrochemical properties of surface modified 5V LiMn1.42Ni0.42Co0.16O4 spinel cathodes in lithium-ion cells, Chem. Mater. 21 (8) (2009) 1695–1707.

[20] Y.F. Yuan, H.M.Wu, S.Y. Guo, J.B. Wu, J.L. Yang, X.L. Wang, J.P. Tu, Preparation, characteristics and electrochemical properties of surface-modified LiMn2O4 by doped LiNi0.05Mn1.95O4, Appl. Surf. Sci. 255 (2008) 2225–2229.

[21] J.-W. Lee, S.-M. Park, H.-J. Kim, Effect of LiNi1/2Mn1/2O2 coating on the electrochemical performance of Li-Mn spinel, Electrochem. Comm. 11 (2009) 1101–1104.

[22] X. Li, Y. Xu, Spinel, LiMn2O4 active material with high capacity retention, Appl. Surf. Sci. 253 (2007) 8592–8596.

[23] M.M. Thackeray, J. Electrochem. Soc. 142 (1995) 255.

[24] M.R. Palacin, Y. Chabre, L. Dupont, M. Hervieu, P. Strobel, G. Rousse, C. Masquelier, M. Anne, G.G. Amatucci, J.-M. Tarascon, J. Electrochem.Soc. 147 (2000) 845.

[25] J. Rodriguez-Carvajal, G. Rousse, C. Masquelier, M. Hervieu, Phys. Rev. Lett. 81 (1998) 4660.

[26] R. Dziembaj, M. Molenda, J. Power Sources 119–121C (2003) 121.

[27] A. Yamada, M. Tanaka, Mater. Res. Bull. 30 (1995) 715.

[28] A. Yamada, M. Tanaka, K. Tanaka, K. Sekai, J. Power Sources 81–82 (1999) 73.

[29] G. Rousse, C. Masquelier, J. Rodriguez-Carvajal, M Hervieu, Electrochem. Solid-State Lett. 2 (1999) 6.

[30] G.G. Amatucci, A. Du Pasquier, A. Blyr, T. Zheng, J.-M. Tarascon, Electrochim. Acta 45 (1999) 255.

[31] J.-M. Tarascon, M. Armand, Nature 414 (2001) 359.

[32] Y.P. Wu, E. Rahm, R. Holze, Electrochim. Acta 47 (2002) 3491.

[33] B. Ammundsen,M. Saijful Islam, D.J. Jones, J. Rozicˇre, J. Power Sources 81–82 (1999) 500.

[34] T. Ohzuku, S. Takeda, M. Iwanaga, J. Power Sources 81–82 (1999) 90.

[35] M. Wakihara, L. Guohua, H. Ikuta, T. Uchida, Solid State Ionics 86–88 (1996) 907

[36] J. Molenda, J. Marzec, K. S ´ wierczek, W. Ojczyk, M. Ziemnicki, P. Wilk, M. Molenda, M. Drozdek, R. Dziembaj, Solid State Ionics 171 (2004)

[37] D. Capsoni, M. Bini, G. Chiodell, V. Massarotti, P. Mustarell, L. Linati, M.C. Mozzati, C.B. Azzoni, Solid State Commun. 126 (2003) 169.

[38] R. Dziembaj, M. Molenda, D. Majda, S. Walas, Solid State Ionics 157 (2003) 81.

[39] K. S ´ wierczek, J. Marzec, M. Marzec, J. Molenda, Solid State Ionics 157(2003) 89.

[40] L. Guohua, H. Ikuta, T. Uchida, M. Wakihara, J. Electrochem. Soc. 143

[41] A. Paolone, A. Sacchetti, T. Corridoni, P. Postorino, R. Cantelli, G. Rousse, C. Masquelier, Solid State Ionics 170 (2004) 135.

[42] B. Ammundsen, G.R. Burns, M.S. Islam, H. Kanoh, J. Roziere, J. Phys. Chem. B 103 (1999) 5175.

[43] C.M. Julien, M. Massot, Mater. Sci. Eng., B 97 (2003) 217. (1996) 178.

[44 M.M.Thackeray, Manganese oxides for lithium batteries, Progress in Solid State Chemistry 25(1997)1–71.

[45] M.M. Thackeray, Y.ShaoHorn, A.J.Kahaian,K.D.Kepler, E. Skinner, J.T.Vaughey, S.A. Hackney Structural fatigue in spinel electrodes in high voltage(4V)Li/LixMn2O4 Cells, Electro-chemicalandSolid-StateLetters1(1998)7–9.

[46] D.Guan, J.A.Jeevarajan, Y.Wang, Enhanced cycleabilityof LiMn2O4 cathodes by atomic layer deposition of nanosized-thin Al2O3 coatings, Nanoscale3(2011)1465–1469.

[47] Y.Xia, M.Yoshio,An investigation of lithium ion insertion into spinel structure LiMnO compounds Journal of The Electrochemical Society 143(1996)825–833.

[48] H.Huang, C.A.Vincent,P.G.Bruce,Correlating capacity loss of Stoichiometric and non stoichiometric lithium manganese oxide spinel electrodes with their structural integrity, Journal of The Electrochemical Society146(1999)3649–3654.

[49] Y.Shin, A.Manthiram, Microstrain and capacity fade in spinel manganese oxides, Electrochemical and Solid-StateLetters5 (2002) A55–A58.

[50] M.Okubo, Y.Mizuno, H.Yamada, J.Kim, E.Hosono, H. Zhou, T.Kudo, I.Honma, FastLi ion insertion into nanosized LiMn2O4 withoutdomainboundaries,ACSNano4(2010)741–752.

[51] H.Xia, H.Wang, W.Xiao, L.Lu, M.O.Lai, Properties of LiNi1/3Co1/3Mn1/3O2 cathode material synthesized by a modified Pechini method for high-power lithium-ion batteries, Journal of Alloys and Compounds 480 (2009)696–701.

[52] H.Xia, M.Lai, L.Lu, Nano flaky MnO2/carbon nanotube Nanocomposites as anode materials for lithium- Ion batteries, Journal ofMaterialsChemistry20(2010)6896–6902.

[53] A.D. Pasquier,A. Blyr, P. Courjal, D. Larcher,G. Amatucci, B. Gerand, J.M. Tarascon,

J. Electrochem. Soc. 146 (1999) 428.

[54] Y. Li, M. Takahashi, B.F.Wang, Electrochim. Acta 51 (2006) 3228.

[55] J. Cho, M.M. Thackeray, J. Electrochem. Soc. 146 (1999) 3577.

[56] J.M. Tarascon, W.R. Mckinnon, T.N. Bowmer, et al., J. Electrochem. Soc. 141 (1994) 1421.

[57] Y.S. Lee, Y.K. Sun, K.S. Nahm, Solid Ionic State 109 (1998) 285.

[58] Ming-shu Zhao,Yu-chun Zhai,Yan-wen Tian, et al., Chin. J. Power Sources 25 (2001) 246.

[59] Fu YP, Su YH, Lin CH, Wu SH. Comparison of the microwave-induced combustion and solid-state reaction for the synthesis of LiMn2O4 powder and their electrochemical properties. Ceram Int 2009;35:3463e8.

[60] Park YJ, Kim JG, Kim MK, Chung HT, Kim G (2000) Solid State Ionics 130:203

[61] Liu W, Farringto GC, Chaput F, Dunn B (1996) J Electrochem Soc 143:879

[62] Sun YK, Oh IH, Kim KY (1997) Ind Eng Chem Res 36:4839

[63] Enhanced capacity retention of Co and Li doubly doped LiMn2O4 ChangyinWang, Shigang Lu∗, Surong Kan, Jing Pang,Weiren Jin, Xiangjun Zhang Energy Materials and Technology Research Institute, General Research Institute for Nonferrous Metals, Beijing 100088, PR China

[64] S. Lee, et al. Angew. Chem. Int. 51 (2012) 8748.